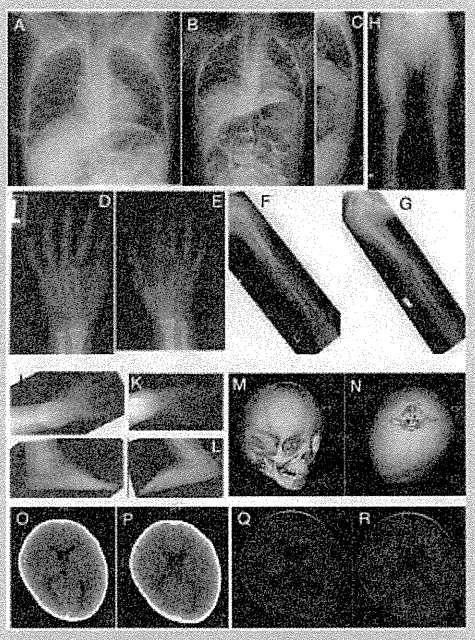


FIG. 3. Radiographs of Patient 1 at age 1 year and 10 months (A) and 2 years and 6 months (B–L). Cranial and brain CT of Patient 1 at age 2 years and 6 months (M–P). Brain MRI of Patient 2 at age 1 year and 10 months (Q, R).

could hardly be flexed or extended. The proximal IP joints in bilateral index to little fingers and the MP joints in all fingers could be flexed and extended, but could not be moved separately and smoothly. His skin was hyperextensible and bruisable. Fine palmar creases were also noted (Fig. 2F). He occasionally had constipation and abdominal pain. A cardiac ultrasonography showed trivial mitral valve prolapse, patent ductus arteriosus, and dextrocardia. A brain MRI showed bilateral ventricular enlargement (Fig. 3Q, R). G-banded chromosomes were normal. His intelligence was normal.

## SKELETAL INVESTIGATIONS

Radiographs of Patient 1 were reviewed. At age 2 years and 6 months, he had mild scoliosis (Fig. 3B), which was not noted at age 1 year and 10 months (Fig. 3A). Physiological lumbar lordosis was not present (Fig. 3C). The left hip joint was dislocated (Fig. 3H). Long bones of the legs and arms showed over modeling, with narrowing diaphysis and widening metaphysis (Fig. 3F–H). Bilateral tibiae and fibulae were medially curved (Fig. 3H). Short bones of the hands (Fig. 3D, E) and feet (Fig. 3I–L) also showed over modeling, as well as osteoporotic changes in the feet (Fig. 3I–L).

## MUTATION ANALYSIS

Genomic DNA was extracted from peripheral blood leukocytes of the patients and their parents, and was amplified with PCR using four primer sets for *CHST14* (sequences available on request). Through direct sequencing of the PCR products, compound heterozygous mutations were detected in both patients: c.842 C > T causing p. Pro281Leu (p.P281L) and c.878 A > G causing p.Tyr293Cys (p.Y293C) in Patient 1; c.626 T > C causing p.Phe209Ser (p.F209S) and c.842 C > T causing p.Pro281Leu (p.Y293C) in Patient 2 (data not shown). The parents had one of the two heterozygous mutations observed in their children.

## DISCUSSION

We have presented detailed clinical characteristics and courses of two new unrelated pediatric patients with compound heterozygous *CHST14* mutations. The features showed striking resemblance to those of patients with EDSKT in their infancy to early childhood [Kosho et al., 2005, 2010]. *CHST14* mutations (P281L/Y293C) in Patient 1 were identical to those found in two patients with EDSKT [Miyake et al., 2010]. F209S found in Patient 2, which was not listed on a database of common gene variations in the Japanese population (JSNP) [Haga et al., 2002], was the mutation that has never found in previous patients with ATCS, EDSKT, or MCEDS.

To date, 22 patients (12 males, 10 females) from 14 families, including present patients, have been reported to have homozygous or compound heterozygous mutations in *CHST14* (Tables I and II) [Dündar et al., 1997; Sonoda and Kouno, 2000; Dündar et al., 2001; Janecke et al., 2001; Yasui et al., 2003; Kosho et al., 2005; Dündar et al., 2009; Kosho et al., 2010; Malfait et al., 2010; Miyake et al., 2010]. Eight families were of Japanese origin, three of Turkish origin, one of Austrian origin, and one of Indian origin. The median patients' age at their initial publication was 4 years and 1 month (range, 0 day–32 years): 7 months (range, 0 day–6 years) in ATCS, 12.5 years in EDSKT (range, 2 years–32 years), and 21 years (range, 12 years–22 years) in MCEDS.

*CHST14* mutations included V49X in two families (ATCS, MCEDS), K69X in one (EDSKT), R135G in one (ATCS), L137Q in one (ATCS), F209S in one (EDSKT), R213P in one (ATCS), P281L in eight (EDSKT), C289S in one (EDSKT), Y293C in four (one ATCS, three EDSKT), and E334GfsX107 in one (MCEDS). Sulfotransferase activity of COS-7 cells transfected with *CHST14* containing K69X, P281L, C289S, or Y293C mutation was decreased at almost the same level, suggesting that loss-of-function mutations in *CHST14*, that is to say D4ST1 deficiency, would cause these disorders [Miyake et al., 2010].

Characteristic craniofacial features at birth to early infancy (large fontanelle, hypertelorism, short and downslanting palpebral fissures, blue sclerae, short nose with hypoplastic columella, low-set and rotated ears, high palate, long philtrum, thin upper lip vermilion, small mouth, and micro-retrognathia) were noted in most patients with ATCS, EDSKT, and MCEDS. Slender and asymmetrical facial shapes with protruding jaws from school age, commonly observed in patients with EDSKT, were also described in ATCS2 at age 15 years, ATCS3 at age 6 years, ATCS7 at age 8 years [Dündar et al., 2009], and in MCEDS1 at age 21 years [Malfait et al., 2010]. A pair of ATCS siblings had palatal defects: ATCS4 with cleft lip and palate, which was surgically repaired, and ATCS5 with cleft soft palate [Sonoda and Kouno, 2000].

Congenital multiple contractures, most specifically adduction–flexion contractures of thumbs and talipes equinovarus,

**TABLE I. Clinical Characteristics of Reported Patients With D4ST1 Deficiency (Continued)**

| | | | | | | Craniofacial | | | | | | | | | | | | | | Skeletal | | | | | | | | | Cutaneous | | | | | | Cardiovascular | | | | Gastrointestinal | | |
|---|---|---|---|---|---|---|---|---|---|---|---|---|---|---|---|---|---|---|---|---|---|---|---|---|---|---|---|---|---|---|---|---|---|---|---|---|---|---|---|---|
| Family | Patient | Origin | *CHST14* Mutations | Age at initial publication (d, days; m, months; y, years) | Sex | Large fontanelle (early childhood) | Hypertelorism | Down-slanting palpebral fissures | Blue sclerae | Short nose with hypoplastic columella | Ear deformities | Palatal abnormalities | Long philtrum and thin upper lip | Small mouth/micro-retrognathia in infancy | Short neck | Slender face/protruding jaw from school age | Facial asymmetricity from school age | Malfunoid habitus/slender build | Congenital multiple contractions | Recurrent/chronic joint dislocations | Pectus deformities | Spinal deformities | Peculiar fingers (tapering – slender and cylindrical) | Progressive talipes deformities | Hyperextensibility/redundancy | Bruisability | Fragility/atrophic scars | Fine/Acrogeria-like palmar creases | Hyperalgesia to pressure | Recurrent subcutaneous infections/fistula | Congenital heart defects | Valve abnormalities | Large subcutaneous hematomas | (Hemo) pneumothorax | Constipation | Others |
| ATCS | | | | | | | | | | | | | | | | | | | | | | | | | | | | | | | | | | | | | | | | |
| 1 | 1 | Turkish | V49X homo | 3.5y | F | + | + | + | + | | P, PR | H | + | | + | | | + | | | | + | | | | | | | | – | | | | | | | | |
| | 2 | | | 1.5y | M | + | + | + | + | + | P, PR | | + | | + | +a | | +a | + | +a | Exa | KSa | + | Planus, valgus# | | | +a | | | – | | | | | | | | |
| | 3 | | | 6y | F | | + | + | | + | P | | + | | | + | + | + | + | | F–T | S | + | Varus | | | | + | | | | | | | | | | |
| 2 | 4 | Japanese | Y293C homo | 4y | M | + | + | + | | + | LS | CL/CP | + | | | | | | + | + | Ca | | + | Planus, valgus | | | | | | | | | | | | | | |
| | 5 | | | 7m | M | + | + | + | | + | LS | CSP | + | | | | | | + | + | | | + | | | | | | | ASD | | | | | | | | |
| 3 | 6 | Austrian | R213P homo | 0d† | M | + | + | + | | | PR, LS | | | | + | | | | + | | | S | + | | | | | | | ASD, CoA | | | | | | | Common mesentery |
| | 7 | | | 12m | M | + | + | + | + | | D, PR | | | | + | +a | | +a | + | | F–Ta | | + | Planus, valgus# | | | +a | | | – | | | | | | | Absence of gastrocolic omentum, spontaneous volvulus of small intestine |
| 4 | 8 | Turkish | R135G / L137Q | 1–4m† | F | | | | | | | | | | | | | | + | | | | | | | | | | | | | | | | | | |
| | 9 | | | 1–4m† | M | | | | | | | | | | | | | | + | | | | | | | | | | | | | | | | | | |
| | 10 | | | 1–4m† | M | | | | | | | | | | | | | | + | | | | | | | | | | | | | | | | | | |
| | 11 | | | 3m | M | + | + | + | + | | D, LS | H | + | | + | | | | + | | | | + | | | | | | | – | | | | | | | |
| MCEDS | | | | | | | | | | | | | | | | | | | | | | | | | | | | | | | | | | | | | | | | |
| 1 | 1 | Turkish | V49X homo | 22y | F | + | | | + | | PR, LS | H | + | | | + | + | + | + | | F–T | KS | + | Planus, valgus | + | + | + | + | | + | – | – | | | | | Hiatal hernia, gastroesphageal reflux, abdominal pain |
| | 2 | | | 21y | F | + | | | + | + | | H | + | | | | | | + | + | F–T | S | + | Small, broad | + | + | + | + | | | | | | | | | |
| 2 | 3 | Indian | E334GfsX107 homo | 12y | F | | | | | + | LS | | – | | | | | + | + | + | | KS | + | Planus, valgus | – | + | + | + | | + | | | | | | | Duodenum obstruction due to malrotation |
| EDSKT | | | | | | | | | | | | | | | | | | | | | | | | | | | | | | | | | | | | | | | | |
| 1 | 1 | Japanese | P281L / Y293C | 11y | F | + | + | + | + | + | LS | H | + | + | | + | + | + | + | + | Ex | KS | + | Planus, valgus | + | + | + | + | + | + | ASD | TR, TVP, MVP | + | – | + | Gastric ulcer§ |
| 2 | 2 | Japanese | P281L homo | 14y | F | + | + | + | + | + | LS | H | + | + | | + | + | + | + | + | F–T | S | + | Cavus, valgus | + | + | + | + | + | + | – | | + | +§ | + | Diverticular perforation§ |
| 3 | 3 | Japanese | P281L homo | 32y | M | + | + | + | + | – | LS | H | + | + | | + | + | + | + | + | F–T | KS | + | Planus, valgus | + | + | + | + | + | + | | AR, ARD, MR | + | + | + | Diverticular perforation |
| 4 | 4 | Japanese | K69X / P281L | 32y | M | | + | | + | | | H | | | | + | + | + | + | + | Ex | KS | + | Planus, valgus | + | + | – | + | – | – | | | + | + | – | |
| 5 | 5 | Japanese | P281L / C289S | 20y | F | + | + | + | + | + | LS | H | + | + | | + | + | + | + | + | Ex | S | + | Planus, valgus | + | + | + | + | + | + | | AR, MR, IE | + | – | + | |
| 6 | 6 | Japanese | P281L / Y293C | 4y | F | + | + | + | + | + | LS | H | + | | | | | | + | | Ex | S | + | Planus | + | + | + | + | + | + | | | + | – | + | |
| Present report (EDSKT) | | | | | | | | | | | | | | | | | | | | | | | | | | | | | | | | | | | | | | | | |
| 7 | 7 | Japanese | P281L / Y293C | 2y | M | + | + | + | + | + | PR, LS | H | + | + | | | | | + | + | | F–T | S | + | Planus, valgus | + | + | + | + | – | + | – | ARD | – | – | + | |
| 8 | 8 | Japanese | F209S / P281L | 6y | M | + | + | + | + | + | PR, LS | H | + | + | | | | | + | + | + | Ex | | + | Planus | + | + | – | + | + | – | PDA | MVP | + | – | + | Abdominal pain |

ATCS, adducted thumb-clubfoot syndrome; EDSKT, Ehlers–Danlos Syndrome, Kosho Type; MCEDS, Musculocontractural Ehlers–Danlos Syndrome
+, present; Blank, information not available; †, died; F, female; M, male; P, prominent; PR, posteriorly rotated; LS, low set; D, dysplastic; H, high; CL, cleft lip; CP, cleft palate; CSP, cleft soft palate;
Ex, excavatum; F–T, flat and thin; Ca, carinatum; KS, kyphoscoliosis; S, scoliosis; ASD, atrial septal defect; CoA, coarctation of aorta; PDA, patent ductus arteriosus;
TR, tricuspid valve regurgitation; TVP, tricuspid valve prolapse; MVP, mitral valve prolapse; AR, aortic valve regurgitation; ARD, aortic root dilation; MR, mitral valve regurgitation; IE, infectious endocarditis
ATCS Patient 1 died at age 6 years [Dündar et al., 2009].
a, Information from reassessment by Dündar et al. [2009], describing ATCS P2 at age 15 years and ATCS P7 at age 8 years
b, Information from reassessment by Kosho et al. [2010], describing EDSKT1 at age 16 years and EDSKT2 at age 32 years

TABLE II. Clinical Characteristics of Reported Patients With D4ST1 Deficiency

| | | Urogenital | | | Ophthalmological | | | | | | | Development | | | Growth (prenatal) | | | | Growth (postnatal) | | | | |
|---|---|---|---|---|---|---|---|---|---|---|---|---|---|---|---|---|---|---|---|---|---|---|---|
| Family | Patient | Nephro (Cysto) lithiasis | Cryptorchidism | Others | Breast development | Strabismus | Refractive errors | Glaucoma/elevated intraocular pressure | Others | Hearing impairment | Ventricular abnormalities (brain) | Gross motor delay | Age of unassisted walk (y, years; m, months) | Mental delay | Gestational weeks | Birth length (centile or SD) | Birth weight (centile or SD) | Birth OFC (centile or SD) | Age (y, years; m, months) | Height (centile or SD) | Weight (centile or SD) | OFC (centile or SD) | References |
| ATCS | | | | | | | | | | | | | | | | | | | | | | | |
| 1 | 1 | | | | | + | | | | | Enl | + | No | + | Term | | | | 3.5y | 25-50th | 50th | 50th | Dündar et al., 1997 |
| | 2 | | | | | + | | + | | | Asym | + | | +c | Term | | | | 1.5y | 50th | 10th | 10–25th | Dündar et al., 1997 |
| | | | | | | | | | | | | | | | | | | | 15ya | 25–50th | <3rd | | Dündar et al., 2009 |
| | 3 | | | | | + | | | | | | | | | | | | | 6y | 10–25th | <3rd | | Dündar et al., 2009 |
| 2 | 4 | | + | Hydronephrosis | | | | | | | | | | – | 39wk | –0.6 | –0.9 | –0.8 | 4y2m | –3.9 | –1.8 | –0.9 | Sonoda and Kouno, 2000 |
| | 5 | | + | Hydronephrosis, inguinal hernia | | | | | | | | | – | – | 38wk | –1.6 | –1.3 | –0.5 | 7m | –2.1 | –1.4 | –1.1 | Sonoda and Kouno, 2000 |
| 3 | 6 | | + | Horseshoe kidney | | | | | | | Enl | | | | 32wk | 25th | 10th | 25th | | | | | Janecke et al., 2001 |
| | 7 | | + | | | + | | | | | Asym | – | | – | 38wk | 50th | 25th | 50th | 8ya | 10-25th | <3rd | | Janecke et al., 2001 |
| | | | | | | | | | | | | | | | | | | | | | | | Dündar et al., 2009 |
| 4 | 8 | | | | | | | | | | | | | | | | | | | | | | Dündar et al., 2001 |
| | 9 | | | | | | | | | | | | | | | | | | | | | | Dündar et al., 2001 |
| | 10 | | | | | | | | | | | | | | | | | | | | | | Dündar et al., 2001 |
| | 11 | + | + | Inguinal hernia | | | | | | | Enl, Asym | | | | | | | | 3m | <3rd | 3–10th | 10th | Dündar et al., 2001 |
| MCEDS | | | | | | | | | | | | | | | | | | | | | | | |
| 1 | 1 | + | | | – | | My | + | Retinal detachment, pthysis bulbi | + | | + | 4y | | 42wk | ±0 | –0.67 | | 22y | –2.0 | | ±0 | Malfait et al., 2010 |
| | 2 | + | | Hydronephrosis, renal ptosis, ureteral stenosis | – | | My | + | Retinal detachment | + | | + | 2y | | 42wk | | | | 14y | +0.68 | | >2.0 | |
| 2 | 3 | | | | | | My | | Microcornea | | | + | | | Term | | –0.88 | | | | | | Malfait et al., 2010 |
| EDSKT | | | | | | | | | | | | | | | | | | | | | | | |
| 1 | 1 | | | Bladder dilation, recurrent UTI, involuntary contractionb | –b | + | Hy | – | Microcornea | + | Enl | + | 2y | +d | 42wk | –0.1 | –1.3 | –1.0 | 7y | +0.8 | –1.0 | ±0 | Kosho et al., 2005 |
| | | | | | | | | | | | | | | | | | | | 11y | +0.2 | –2 | +0.2 | Kosho et al., 2010 |
| | | | | | | | | | | | | | | | | | | | 16y | +0.3 | –0.4 | +0.2 | |
| 2 | 2 | + | | Atonic bladder, recurrent UTI | –b | + | My, As | +b | | + | | + | No | – | Term | | –2.0 | | 15y | –3.2 | | | Kosho et al., 2005 |
| | | | | | | | | | | | | | | | | | | | | | | | Kosho et al., 2010 |
| 3 | 3 | | + | Hypogonadism | | + | My, As | – | Microphthalmia | + | | + | | – | 40wk | +1.3 | +0.5 | +0.8 | 30y | +1.2 | –1.7 | | Kosho et al., 2010 |
| 4 | 4 | | | | | – | – | – | Retinal detachment | – | | | | + | | | | | 23y | –0.4 | –2.4 | | Yasui et al., 2003 |
| | | | | | | | | | | | | | | | | | | | | | | | Kosho et al., 2010 |
| 5 | 5 | + | | Delayed menarche, irregular menstruation | – | + | My, As | + | | – | | + | 2y2m | – | 39wk | –1.1 | –0.4 | +1.0 | 19y | –0.1 | –0.8 | | Kosho et al., 2010 |
| 6 | 6 | | | | | + | My, As | + | | + | | + | 1y5m | – | 41wk | –1.2 | –0.5 | –0.6 | 4y | –1.2 | –1.3 | –0.9 | Kosho et al., 2010 |
| Present report | | | | | | | | | | | | | | | | | | | | | | | |
| 7 | 7 | | + | | | + | Hy, As, Am | – | | | | + | No | + | 38wk3d | –1.3 | +0.2 | +0.4 | 2y | –2.2 | –2.4 | –1.2 | Patient 1 |
| 8 | 8 | | + | | | + | | | | – | Enl | + | 2y6m | – | 38wk | +0.3 | +0.3 | –0.5 | 6y | –0.7 | –1.4 | +0.1 | Patient 2 |

ATCS, adducted thumb-clubfoot syndrome; EDSKT, Ehlers-Danlos Syndrome, Kosho Type; MCEDS, Musculocontractural Ehlers-Danlos Syndome
+, present; Blank, information not available; UTI, urinary tract infection; Hy, hyperopia; My, myopia; As, astigmatism; Am, amblyopia; Enl, enlargement; Asym, asymmetry; No, not ambulant
a, Information from reassessment by Dündar et al. [2009], describing ATCS P2 at age 15 years and ATCS P7 at age 8 years.
b, Information from reassessment by Kosho et al. [2010], describing EDSKT1 at age 16 years and EDSKT at age 32 years.
c, IQ was 91 at Porteus test and 86 at Goodenough test at age 7 years and 2 months [Janecke et al., 2001].
d, mild learning dissability

were cardinal features in patients with ATCS, EDSKT, and MCEDS. Peculiar fingers described as "tapering," "slender," and "cylindrical" were also common features. Aberrant finger movement was described in EDSKT1 [Kosho et al., 2010], EDSKT7, and EDSKT8. EDSKT1, EDSKT2, EDSKT3, and EDSKT5 were found to have tendon abnormalities such as anomalous insertions of flexor muscles, which might result in contractures [Kosho et al., 2005, 2010]. In childhood, spinal deformities (scoliosis, kyphoscoliosis) and talipes deformities (planus, valgus) occurred and progressed. Malfanoid habitus, recurrent joint dislocations, and pectus deformities (flat and thin, excavatum, carinatum) were also evident. Talipes equinovarus in seven EDSKT patients and MCEDS3 was surgically repaired [Kosho et al., 2005, 2010; Malfait et al., 2010]. EDSKT3 received tendon transplantations for defects of tendons to bilateral thumbs, and EDSKT4 received surgical fixation of bilateral ankle joints as well as surgery for carpal tunnel syndrome [Kosho et al., 2010]. MCEDS1 underwent surgery for rapidly worsened kyphoscoliosis at age 14 years [Malfait et al., 2010].

Bone mineral density (BMD) was decreased in ATCS2 at age 15 years (Z score −1.6), ATCS3 at age 6 years (Z score −4.6) [Dündar et al., 2009], EDSKT2 at age 29 years (Z score −2.4 for the lumbar spine 1–4, −2.3 for the 33% radius), and EDSKT3 at age 31 years (Z score −3.7 for the lumbar spine 1–4, −3.6 for the femoral neck) [unpublished data], whereas BMD was normal in ATCS7 at age 8 years [Dündar et al., 2009] and EDSKT1 at age 15 years (Z score +1.6 for the lumbar spine 1–4, −0.9 for the femoral neck) [unpublished data]. Urine N-telopeptide of collagen type I (NTX), an osteoclast marker, was increased at 92.8 nmol BCE/mmol Cr in EDSKT1 at age 16 years, 70.3 nmol BCE/mmol Cr in EDSKT2 at age 28 years, and 238.4 nmol BCE/mmol Cr in EDSKT3 at age 31 years [unpublished data] (normal values for premenopausal females, 9.3–54.3; males, 13.0–66.2), whereas serum bone specific alkaline phosphatase (BAP), an osteoblast marker, was normal at 12.5 U/L in EDSKT1 at age 16 years, 25.6 U/L in EDSKT2 at age 28 years, and 15.1 U/L in EDSKT3 at age 31 years (normal values, 9.6–35.4) [unpublished data]. These results in biochemical markers of bone turnover suggested an increase in osteoclast activity with normal osteoblast activity, which could cause oeteopenia or osteoporosis.

Radiologically, diaphysial narrowing of phalanges and metacarpals was noted in EDSKT1 at age 11 and 16 years, EDSKT2 at age 10 and 28 years, EDSKT3 at age 31 years, EDSKT5 at age 19 years [Kosho et al., 2005, 2010], and EDSKT7 at age 2 years and 6 months. Talipes valgus and planus or cavum, with diaphysial narrowing of phalanges and metatarsals, were noted in ATCS7 at age 8 years [Dündar et al., 2009], EDSKT1 at age 11 and 16 years, EDSKT2 at age 14 and 28 years, EDSKT6 at age 4 years [Kosho et al., 2005, 2010], and EDSKT7 at age 2 years and 6 months. Tall vertebral bodies were noted in EDSKT1 at age 11 and 16 years, EDSKT2 at age 14 and 28 years, EDSKT3 at age 31 years, EDSKT4 at age 31 years, EDSKT5 at age 19 years [Kosho et al., 2005, 2010], and MCEDS2 at age 21 years [Malfait et al., 2010], whereas they were not noted in EDSKT6 at age 2 years [Kosho et al., 2010] and EDSKT7 at age 2 years and 6 months.

Cutaneous features were common in most patients with EDSKT and MCEDS, including hyperextensibility to redundancy, bruisability, fragility leading to atrophic scars, acrogeria-like fine palmar creases or wrinkles, hyperalgesia to pressure, and recurrent subcutaneous infections with fistula formation, which lead to skin defects including decubitus necessitating plastic surgery in EDSKT2 [Kosho et al., 2005, 2010]. Excessive palmar creases were observed in ATCS2, ATCS3, and ATCS7, and delayed wound healing and ecchymoses were also recorded ATCS patients [Dündar et al., 2009]. Palmar creases increased and became deeper according to the ages, as compared among photographs of EDSKT1 at age 11 and 16 years, EDSKT2 at age 5 years and 32 years, EDSKT3 at age 32 years, EDSKT5 at age 19years, and EDSKT6 at age 4 years [Kosho et al., 2005, 2010].

Seven patients with EDSKT suffered from large subcutaneous hematomas, which sometimes progressed acutely and massively to be treated intensively (admission, blood transfusion, surgical drainage). These lesions were supposed to be caused by rupture of subcutaneous arteries or veins. Hematoma formation was mentioned in a follow-up observation of ATCS patients [Dündar et al., 2009]. Bleeding time was prolonged in ATCS7 (9 min) [Dündar et al., 2009] and EDSKT4 (11 min) [Yasui et al., 2003; Kosho et al., 2010], whereas it was normal in EDSKT1 (3 min) [Kosho et al., 2005], EDSKT3 (1 min) [unpublished data], and EDSKT7 (1.3 min). EDSKT1 had, to prevent large subcutaneous hematomas, intranasal administration of 1-desamino-8-D-arginine vasopressin (DDAVP) after injuries [Kosho et al., 2005, 2010]. A large hematoma over the buttocks in EDSKT4 was treated with intranasal DDAVP and intramuscular conjugated estrogen [Yasui et al., 2003; Kosho et al., 2010].

Two ATCS and two EDSKT patients had congenital heart defects (atrial septal defect was the most common, observed in three), and five EDSKT patients had cardiac valve abnormalities. EDSKT5 suffered from infectious endocarditis probably resulting from aortic valve or mitral valve regurgitation, and underwent surgery. Three adult patients with EDSKT developed pneumothorax or hemopneumothorax, treated with chest tube drainage; and two of them suffered from diverticular perforation, treated surgically. Various gastrointestinal abnormalities were observed: Constipation in seven EDSKT patients and abdominal pain in one EDSKT and one MCEDS patients, as well as common mesentery in ATCS6, absent gastrocolic omentum and spontaneous volvulus of small intestine in ATCS7, gastric ulcer necessitating partial gastrectomy in EDSKT1, and duodenum obstruction due to malrotation treated surgically in MCEDS3 [Janecke et al., 2001; Dündar et al., 2009; Kosho et al., 2010; Malfait et al., 2010].

Urological complications included nephrolithiasis or cystolithiasis in one ATCS, two EDSKT, and two MCEDS patients; hydronephrosis in two ATCS and one MCEDS patients, dilated or atonic bladder with recurrent urinary tract infection in two EDSKT patients, and horseshoe kidney in one ATCS patient. Hydronephrosis in MCEDS2 was caused by renal ptosis and ureteral stenosis, for which a ureteral stent was placed with a laparoscopic procedure, complicated by severe hemorrhage due to excessive tissue fragility [Malfait et al., 2010].

Cryptorchidism was observed in five ATCS and three EDSKT male patients. EDSKT3, who received orchiopexy, showed hypogonadism in adulthood. In female patients older than adolescence, poor breast development was noted in three EDSKT (EDSKT1 and

EDSKT2 showed normal menstruation cycles; EDSKT5 showed delayed menarche and irregular menstruation cycles) and two MCEDS patients. No female patients have been reported to be pregnant.

Various ophthalmological complications were observed: Strabismus in four ATCS and seven EDSKT patients, refractive errors in six EDSKT and three MCEDS patients, glaucoma or elevated intraocular pressure in one ATCS, three EDSKT, and two MCEDS patients; microcornea or microphthalmia in two EDSKT and one MCEDS patients, and retinal detachment in one EDSKT and two MCEDS. Retinal detachment in EDSKT4 [Kosho et al., 2010] and glaucoma in MCEDS1 [Malfait et al., 2010] required surgery. Hearing impairment was noted in four EDSKT patients (predominantly for high-pitched sound in EDSKT1, EDSKT2, and EDSKT6) and two MCEDS.

Gross motor developmental delay was observed in two ATCS, seven EDSKT, and three MCEDS patients; and ages of unassisted walk in patients who accomplished it ranged from 1 year and 5 months to 4 years (median, 2 years and 1 month). EDSKT2, at age 32 years, could not walk unassisted because of severe foot deformities and muscle weakness of the legs [Kosho et al., 2010]. An underlying myopathic process was suggested in ATCS2 because of reduced amplitude muscle action potentials with normal distal latency time and nerve conduction velocity, whereas muscle biopsy did not reveal any histological abnormality [Dündar et al., 1997]. Mild mental delay was suggested in two ATCS and two EDSKT patients. ATCS2 was reported to have global psychomotor delay at the initial publication [Dündar et al., 1997], whereas his IQ was around 90 at age 7 years and 2 months [Janecke et al., 2001]. Five ATCS and two EDSKT patients showed ventricular enlargement and/or asymmetry on brain ultrasonography, CT or MRI. ATCS7 also showed absence of the left septum pellucidum [Janecke et al., 2001]. EDSKT6 had tethering of a spinal cord, and underwent duraplasty [Kosho et al., 2010].

Growth assessment was performed using data described with SD scores, excluding data described with centile scores. Patients with *CHST14* mutations showed mild prenatal growth retardation: The mean birth length −0.5 SD and the median −0.6 SD (n = 9; range, −1.6 SD to +1.3 SD); the mean birth weight −0.6 SD and the median −0.67 SD (n = 11; range, −2.0 SD to +0.5 SD); and the mean birth OFC −0.2 SD and the median −0.5 SD (n = 8; range, −1.0 SD to +1.0 SD). Postnatal growth was also mildly impaired with slenderness and relative macrocephaly: The mean height −0.9 SD and the median −0.6 SD (14 data from 12 patients; range, −3.9 SD to +1.2 SD); the mean weight −1.5 SD and the median −1.4 SD (11 data from 9 patients; range, −2.4 SD to −0.4 SD); the mean OFC −0.2 SD and the median ±0 SD (10 data from 8 patients; range, −1.2 SD to >2.0 SD).

Light microscopic investigations on skin specimens from EDSKT5 and EDSKT6 showed that fine collagen fibers were predominant in the reticular to papillary dermis and normally thick collagen bundles were markedly reduced [Miyake et al., 2010]. Electron microscopic investigations of the specimens showed that collagen fibrils were dispersed in the reticular dermis, compared with regularly and tightly assembled ones observed in the control, whereas each collagen fibril was smooth and round, not varying in size and shape, similar to each fibril of the control [Miyake et al., 2010]. These findings suggested that the main pathological basis of this disorder would be insufficient assembly of collagen fibrils, compatible with the evidence that dermatan sulfate of decorin proteoglycan, a key regulator of collagen fibril assembly that contains both chondroitin sulfate and dermatan sulfate in its glycosaminoglycan chains and controls the distance between collagen fibrils, was found to be completely lost and replaced by chondroitin sulfate in patients' fibroblasts [Miyake et al., 2010]. However, both light microscopic and electron microscopic findings of skin were assessed as normal in ATCS7 [Dündar et al., 2009]. In MCEDS2, most collagen bundles were small-sized, some of which were composed of variable diameter collagen fibrils separated by irregular interfibrillar spaces [Malfait et al., 2010].

This comprehensive review of the patients with loss-of-function mutations in *CHST14* (D4ST1 deficiency) supports the notion that ATCS, EDSKT, and MCEDS would be a single clinical entity with variable inter- and intra-familial expressions and with different presentations depending on the patients' ages at diagnosis or at publication. The disorder, we preferably would like to coin simply as EDS due to D4ST1 deficiency or D4ST1 deficient EDS (DD-EDS), is a clinically recognizable syndrome, characterized by progressive multisystem fragility-related manifestations including joint dislocations and deformities, skin hyperextensibility, bruisability, and fragility; recurrent large subcutaneous hematomas, and other cardiac valvular, respiratory, gastrointestinal, and ocular complications, which are considered to result from connective tissue weakness and be consequences of insufficient decorin-mediated assembly of collagen fibrils caused by D4ST1 deficiency. The disorder also shows various malformations including distinct craniofacial features, multiple congenital contractures, and congenital defects in cardiovascular, gastrointestinal, renal, ocular, and central nervous systems, which might not simply be accountable for connective tissue weakness but could be considered as inborn errors of development. In a recent review focusing on ATCS, Zhang et al. [2010] state that D4ST1 deficiency is the only recognized condition resulting from a defect specific to DS biosynthesis, and that the disorder emphasizes the roles D4ST1 play in human development and extracellular matrix maintenance.

DD-EDS could be detected at birth from characteristic craniofacial and skeletal features and molecular genetic testing gives definitive diagnosis. Initial screening for congenital cardiac, ocular, and renal abnormalities and hearing loss would be necessary. In infancy, orthopedic intervention for talipes equinovarus (serial plaster casts, surgery) as well as physical therapy for motor developmental delay would be the center of management. Laxatives and/or enema are considered in patients with constipation. Surgical fixation is considered for cryptorchidism in males. Regular follow-up for ophthalmological (strabismus, refractive errors, glaucoma), otological (otitis media with effusion, hearing loss), urological (urination, bladder enlargement), and cardiovascular (valve abnormalities, aortic root dilation) problems should be continued. After walking independently, attention should be paid to progressive foot deformities and trauma that could cause skin lacerations, joint dislocations, and massive subcutaneous hematomas. Intranasal DDAVP after injuries is considered to prevent large subcutaneous hematomas. From adolescence, assessment of spinal deformities (scoliosis, kyphoscoliosis) and secondary sex

characteristics (breast development in females and gonadal function in males) would be necessary. In adulthood, appropriate treatments should be performed on occasional emergency complications ([hemo]peumothorax, diverticular perforation). Wrist-type sphygmomanometer would be suitable for patients with hyperalgesia to pressure [unpublished observation].

Very recently, Janecke et al. [2011] have claimed that it would lead to confusion for clinicians and researchers to categorize the D4ST1 deficiency into a type of EDS and that an appropriate term should be "Dermatan sulfate-deficient adducted thumb-clubfoot syndrome." The reasons were described as follows: Clinically, "adducted thumb" and "clubfoot" would be the most distinguishable features at birth; etiologically, the molecular basis would differ substantially from EDS. In reply to the article, we have presented sufficient evidences for categorizing the disorder into a type of EDS: Clinically, the disorder would satisfy all the hallmarks of EDS (skin hyperextensibility, joint hypermobility, and tissue fragility affecting the skin, ligaments, joints, blood vessels, and internal organs), and the patients should be treated as having generalized connective tissue fragility in the lifelong management; etiologically, multisystem fragility in the disorder was found to be caused by impaired assembly of collagen fibrils caused by dermatan sulfate loss in the decorin glycosaminoglycan chain [Kosho et al., submitted].

In conclusion, ATCS, EDSKT, and MCEDS; which were found independently to be caused by D4ST1 deficiency, would be a single clinical entity with variable expressions and with different presentations depending on the patients' ages. The syndrome is characterized by a unique set of clinical features including progressive multisystem fragility-related manifestations (joint dislocations and deformities, skin hyperextensibility, bruisability, and fragility; recurrent large subcutaneous hematomas, and other cardiac valvular, respiratory, gastrointestinal, and ocular complications) resulting from impaired assembly of collagen fibrils, as well as various malformations (craniofacial features, multiple congenital contractures, and congenital defects in cardiovascular, gastrointestinal, renal, ocular, and central nervous systems) resulting from inborn errors of development.

## ACKNOWLEDGMENTS

The authors express their gratitude to the patients and their families for participating in this study. They are also thankful to Dr. Inaba (Department of Pediatrics, Shinshu University School of Medicine) for his comments on a neurological assessment and Miss Kunimi for her technical assistance. This work was mainly supported by Research on Intractable Diseases from Japanese Ministry of Health, Welfare, and Labor (#2141039040) (N.O., N. Miyake, Y.F., N. Matsumoto, T.K.).

## REFERENCES

Cheng S, Maeda T, Yamagata Z, Tomiwa K, Yamakawa N. Japan Children's Study Group. 2010. Comparison of factors contributing to developmental attainment of children between 9 and 18 months. J Epidemiol 20:S452–S458.

Dündar M, Demiryilmaz F, Demiryilmaz I, Kumandas S, Erkilic K, Kendirch M, Tuncel M, Ozyazgan I, Tolmie JL. 1997. An autosomal recessive adducted thumb-club foot syndrome observed in Turkish cousins. Clin Genet 51:61–64.

Dündar M, Kurtoglu S, Elmas B, Demiryilmaz F, Candemir Z, Ozkul Y, Durak AC. 2001. A case with adducted thumb and club foot syndrome. Clin Dysmorphol 10:291–293.

Dündar M, Müller T, Zhang Q, Pan J, Steinmann B, Vodopiutz J, Gruber R, Sonoda T, Krabichler B, Utermann G, Baenziger JU, Zhang L, Janecke AR. 2009. Loss of dermatan-4-sulfotransferase 1 function results in adducted thumb-clubfoot syndrome. Am J Hum Genet 85:873–882.

Evers MR, Xia G, Kang HG, Schachner M, Baeziger JU. 2001. Molecular cloning and characterization of a dermatan-specific *N*-acetylgalactosamine 4-O-sulfotransferase. J Biol Chem 276:36344–36353.

Haga H, Yamada R, Ohnishi Y, Nakamura Y, Tanaka T. 2002. Gene-based SNP discovery as part of the Japanese Millennium Genome Project: Identification of 190,562 genetic variations in the human genome. J Hum Genet 47:605–610.

Janecke AR, Unsinn K, Kreczy A, Baldissera I, Gassner I, Neu N, Utermann G, Müller T. 2001. Adducted thumb-club foot syndrome in sibs of a consanguineous Austrian family. J Med Genet 38:265–269.

Janecke AR, Baenziger JU, Müller T, Dündar M. 2011. Letter to the Editors. Loss of dermatan-4-sulfotransferase 1 (D4ST1/*CHST14*) function represents the first dermatan sulfate biosynthesis defect, "Dermatan sulfate-deficient adducted thumb-clubfoot syndrome." Hum Mutat 32:484–485.

Kosho T, Takahashi J, Ohashi H, Nishimura G, Kato H, Fukushima Y. 2005. Ehlers-Danlos syndrome type VIB with characteristic facies, decreased curvatures of the spinal column, and joint contractures in two unrelated girls. Am J Med Genet Part A 138A:282–287.

Kosho T, Miyake N, Hatamochi A, Takahashi J, Kato H, Miyahara T, Igawa Y, Yasui H, Ishida T, Ono K, Kosuda T, Inoue A, Kohyama M, Hattori T, Ohashi H, Nishimura G, Kawamura R, Wakui K, Fukushima Y, Matsumoto N. 2010. A new Ehlers-Danlos syndrome with craniofacial characteristics, multiple congenital contractures, progressive joint and skin laxity, and multisystem fragility-related manifestations. Am J Med Genet Part A 152A:1333–1346.

Kosho T, Miyake N, Mizumoto S, Hatamochi A, Fukushima Y, Sugahara K, Matsumoto N. 2011. A response to: Loss of dermatan-4-sulfotransferase 1 (D4ST1/*CHST14*) function represents the first dermatan sulfate biosynthesis defect, "Dermatan sulfate-deficient adducted thumb-clubfoot syndrome". Which name is appropriate, "adducted thumb-clubfoot syndrome" or "Ehlers-Danlos syndrome"? (submitted).

Malfait F, Syx D, Vlummens P, Symoens S, Nampoothiri S, Hermanns-Lê Van Lear L, De Paepe A. 2010. Musculocontractural Ehlers-Danlos syndrome (former EDS type VIB) and adducted thumb clubfoot syndrome (ATCS) represent a single clinical entity caused by mutations in the dermatan-4-sulfotransferase 1 encoding *CHST14* gene. Hum Mutat 31:1233–1239.

Mikami T, Mizumoto S, Kago N, Kitagawa H, Sugahara K. 2003. Specificities of three distinct human chondroitin/dermatan N-acetylgalactosamine 4-O-sulfotransferases demonstrated using partially desulfated dermatan sulfate as an acceptor: Implication of differential roles in dermatan sulfate biosynthesis. J Biol Chem 278:36115–36127.

Miyake N, Kosho T, Mizumoto S, Furuichi T, Hatamochi A, Nagashima Y, Arai E, Takahashi K, Kawamura R, Wakui K, Takahashi J, Kato H, Yasui H, Ishida T, Ohashi H, Nishimura G, Shiina M, Saitsu H, Tsurusaki Y, Doi H, Fukushima Y, Ikegawa S, Yamada S, Sugahara K, Matsumoto N. 2010. Loss-of-function mutations of *CHST14* in a new type of Ehles-Danlos syndrome. Hum Mutat 31:966–974.

Sonoda T, Kouno K. 2000. Two brothers with distal arthrogryposis, peculiar facial appearance, cleft palate, short stature, hydronephrosis,

retentio testis, and normal intelligence: A new type of distal arthrogryposis? Am J Med Genet 91:280–285.

Trowbridge JM, Gallo RL. 2002. Dermatan sulfate: New functions from an old glycosaminoglycan. Glycobiol 12:117R–125R.

Yasui H, Adachi Y, Minami T, Ishida T, Kato Y, Imai K. 2003. Combination therapy of DDAVP and conjugated estrogens for a recurrent large subcutaneous hematoma in Ehlers-Danlos syndrome. Am J Hematol 72:71–72.

Zhang L, Müller T, Baenziger JU, Janecke AR. 2010. Congenital disorders of glycosylation with emphasis on loss of dermatan-4-sulfotransferase? Prog Mol Biol Transl Sci 93:289–307.

CLINICAL GENETICS An International Journal of Genetics, Molecular and Personalized Medicine

Clin Genet 2011: 80: 161–166
Printed in Singapore. All rights reserved



CLINICAL GENETICS
doi: 10.1111/j.1399-0004.2011.01721.x

## Short Report

# Exome sequencing of two patients in a family with atypical X-linked leukodystrophy

Tsurusaki Y, Okamoto N, Suzuki Y, Doi H, Saitsu H, Miyake N, Matsumoto N. Exome sequencing of two patients in a family with atypical X-linked leukodystrophy.
Clin Genet 2011: 80: 161–166. © John Wiley & Sons A/S, 2011

We encountered a family with two boys similarly showing brain atrophy with reduced white matter, hypoplasia of the brain stem and corpus callosum, spastic paralysis, and severe growth and mental retardation without speaking a word. The phenotype of these patients was not compatible with any known type of syndromic leukodystrophy. Presuming an X-linked disorder, we performed next-generation sequencing (NGS) of the transcripts of the entire X chromosome. A single lane of exome NGS in each patient was sufficient. Six potential mutations were found in both affected boys. Two missense mutations, including c.92T>C (p.V31A) in *L1CAM*, were potentially pathogenic, but this remained inconclusive. The other four could be excluded. Because the patients did not show adducted thumbs or hydrocephalus, the *L1CAM* change in this family can be interpreted as different scenarios. Personal genome analysis using NGS is certainly powerful, but interpretation of the data can be a substantial challenge requiring a lot of tasks.

### Conflict of interest

None of the authors have any conflicts of interest to disclose.

**Y Tsurusaki[a], N Okamoto[b], Y Suzuki[c], H Doi[a], H Saitsu[a], N Miyake[a] and N Matsumoto[a]**

[a]Department of Human Genetics, Yokohama City University Graduate School of Medicine, Kanazawa-ku, Yokohama, Japan, and [b]Department of Medical Genetics, and [c]Department of Pediatric Neurology, Osaka Medical Center and Research Institute for Maternal and Child Health, Murodo-cho, Izumi, Japan

Key words: atypical phenotype – exome sequencing – *L1CAM* – X-linked leukodystrophy

Corresponding author: Naomichi Matsumoto, Department of Human Genetics, Yokohama City University Graduate School of Medicine, 3-9 Fukuura, Kanazawa-ku, Yokohama 236-0004, Japan.
Tel.: +81-45-787-2606;
fax: +81-45-786-5219;
e-mail: naomat@yokohama-cu.ac.jp

Received 4 May 2011, revised and accepted for publication 31 May 2011

Focused/selected gene and genomic characterization has usually been carried out in clinically homogeneous groups of multiple affected samples to make identification of genetic abnormalities more efficient. Microarrays and next-generation sequencing (NGS) have provided new avenues for human genetic research (1–6). Using such new technologies, researchers are able to analyze small numbers of patients on a genome-wide scale. Even very rare cases (such as when only a few compatible patients are available or atypical patients showing no similar phenotypes) can be realistic targets of genetic research, as the new technologies can identify aberrations in a single gene from within virtually the whole genome; this could not be achieved with conventional techniques.

We encountered a family with two affected males showing atypical leukodystrophy. The phenotype of these patients did not match any known type of syndromic leukodystrophy. Because we presumed that abnormality of an X-linked gene caused the atypical leukodystrophy in this family, we performed exome sequencing of most of the X-chromosome transcripts and identified an unexpected gene mutation in these patients.

### Materials and methods

#### A family with atypical X-linked leukodystrophy

Two brothers, II-1 currently aged 19 years and II-2 currently aged 17 years, who have unrelated healthy parents, presented with similar clinical

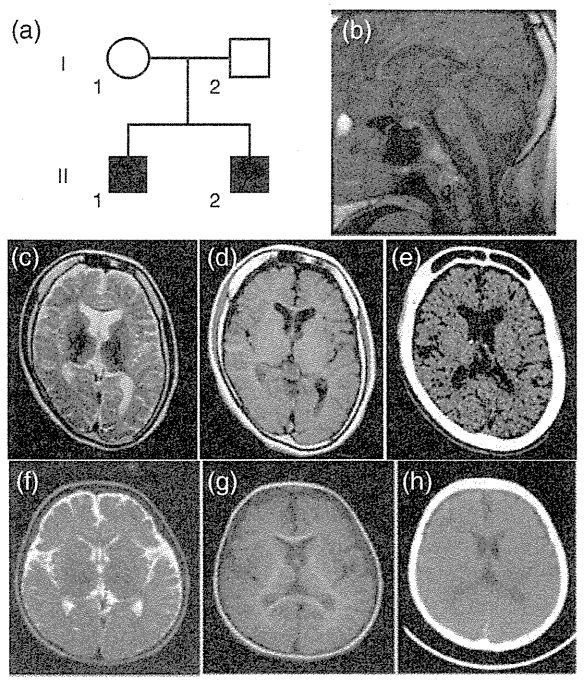


*Fig. 1.* Clinical features of the family. Familial pedigree (**a**). Brain magnetic resonance imaging (MRI) (**b**: T1-weighted image, **c**: T2-weighted image, **d**: T1-weighted image) of individual II-1 at 16 years old showing hypoplasia of the white matter, the brain stem and the corpus callosum. Brain computed tomographic (CT) images of individual II-1 at 19 years old (**e**) indicating a thick calvarium with enlarged frontal sinus as well as calcification of the choroid plexus in the atrophic brain. Brain MRI (**f**: T2-weighted image, **g**: T1-weighted image) of individual II-2 at 2 years old, also displaying hypoplasia of the white matter. Brain CT image of individual II-2 at 5 years old (**h**), also showing a thick calvarium.

features. Their mother did not show any neurological abnormalities (Fig. 1a).

*Patient II-1*

Patient II-1's birth weight was 2840 g at 40 weeks of gestational age. He had congenital nystagmus. He sat unsupported at 7 months old but after this his developmental milestones were delayed. He could creep at 18 months old. Spastic paralysis, especially in the lower extremities, became apparent. He was unable to stand unsupported. His mental development was severely delayed, and he needed special education from elementary school. He had suffered generalized epileptic seizures since he was 10 years old. He was confined to a wheelchair. He had severe mental retardation without speaking a word. His developmental quotient (DQ) at 9 years old was 19 by the Japanese standard method. Severe growth retardation [143 cm (<3%), 24 kg (<3%), occipitofrontal head circumference 49 cm (<3%) at 19 years] was also noted. He did not have dysmorphic features. Blood analysis revealed microcytic anemia [hemoglobin (Hb) 13.4 g/dl, mean corpuscular volume (MCV) (of red blood cell) 70.4 fl (normal: 89–99 fl), mean corpuscular hemoglobin (MCH) (of red blood cell) 23.1 pg (normal: 29–35 pg)] without any evidence of hemolysis or iron deficiency. Hormonal examination indicated that the levels of luteinizing hormone, follicle-stimulating hormone, and thyroid-stimulating hormone were all low [0.9 mIU/ml (normal: 1.2–8.0 mIU/ml), 2.5 mIU/ml (normal: 2.3–15.1 mIU/ml), <0.01 μIU/ml (normal: 0.5–5.0 μIU/ml), respectively]. He showed delayed puberty with small testes. Pubic hair only appeared at 17 years old. His bone age at 18 years old was 12.6 years (67%). Brain magnetic resonance imaging (MRI) at 16 years old revealed brain atrophy associated with reduced white matter and hypoplasia of the brain stem and the corpus callosum (Fig. 1b–d). No hydrocephalus or adducted thumb was observed. Brain computed tomography (CT) at 19 years old showed a thick calvarium with enlarged frontal sinus as well as calcification of the cerebellar tentorium and the choroid plexus (Fig. 1e).

*Patient II-2*

Patient II-2's birth weight was 2910 g at 37 weeks of gestational age. Developmental delay was apparent since he was 10 months old. Spastic paralysis (especially in the lower extremities), confinement to a wheelchair, severe mental retardation without speaking a word (DQ = 5 at 17 years old), and severe growth retardation [130 cm (<3%) and 27 kg (<3%) at 17 years] were phenotypes shared with his brother (II-1). Blood analysis revealed microcytic anemia (Hb 12.0 g/dl, MCV 61.1 fl, MCH 19.0 pg) without any evidence of hemolysis or iron deficiency. Hormonal examination indicated that the levels of luteinizing hormone, follicle-stimulating hormone, and thyroid-stimulating hormone were relatively low (1.9 mIU/ml, 4.2 mIU/ml, <0.23 μIU/ml, respectively). He also showed delayed puberty with small testes. Pubic hair appeared only at 17 years old. His bone age at 17 years old was 11 years (65%). Brain MRI at 2 years old revealed brain atrophy associated with reduced white matter and hypoplasia of the brain stem and corpus callosum (Fig. 1f,g). Brain CT at 5 years old showed a thick calvarium (Fig. 1h). No hydrocephalus or adducted thumb was observed. Most of the clinical features were similar to those of his brother except for the absence of nystagmus in patient II-2.

### Genome-wide SNP genotyping

Genome-wide single-nucleotide polymorphism (SNP) genotyping was performed on individuals I-2, II-1, and II-2 using a GeneChip™ Human Mapping 10K Array Xba 142 2.0 (Affymetrix, Inc., Santa Clara, CA), according to the manufacturer's protocols. Mendelian error in the pedigree to exclude conflicted SNPs was checked using GCOS 1.2 (GeneChip Operating Software; Affymetrix) and batch analysis in GTYPE 4.0 (GeneChip Genotyping Analysis Software; Affymetrix), with the default setting for the mapping algorithm. The linked region, with SNP genotypes shared between individuals II-1 and II-2, was checked manually.

### Genomic partitioning, short-read sequencing, and sequence alignment

Three micrograms of genomic DNA from the affected brothers (II-1 and II-2) was processed using a SureSelect X Chromosome test kit (1582 transcripts covering 3053 kb) (Agilent Technologies, Santa Clara, CA), according to the manufacturer's instructions. Captured DNAs were analyzed using an Illumina GAIIx (Illumina, Inc., San Diego, CA). We used only one of the eight lanes in the flow cell (Illumina) for paired-end, 76-bp reads per sample. Image analysis and base-calling were performed using sequence control software (SCS) real-time analysis and off-line BASECALLER software v1.8.0 (Illumina). Reads were aligned to the human reference genome (UCSC hg19, NCBI build 37.1) using the ELANDv2 algorithm in CASAVA_v1.7.0 (Illumina). The ELANDv2 algorithm can align 100-bp reads to a reference sequence and split the reads into multiple seeds.

### Mapping strategy and variant annotation

Approximately 57.5 million reads from individual II-1 and 71.1 million reads from individual II-2 that passed the quality control (Path Filter) were mapped to the human reference genome using mapping and assembly with quality (MAQ) (7) (Fig. 2). MAQ was able to align 51 720 952 and 65 990 660 reads to the whole genome for individuals II-1 and II-2, respectively; these were then statistically analyzed for coverage using a script created by BITS Co., Ltd. (Tokyo, Japan). SNPs and insertions/deletions were extracted from the alignment data using an original script created by BITS Co., Ltd., along with information on the registered SNPs (dbSNP 131). A consensus quality score of 40 or more was used for the SNP analysis in MAQ. SNPs in MAQ-passed reads were annotated using the SeattleSeq website (http://gvs.gs.washington.edu/SeattleSeqAnnotation/). Variants found by each informatics method were selected in terms of location on chromosome X, unregistered variants (excluding registered SNPs), variants in known genes, variants in coding regions, variants excluding synonymous changes, and variants with an allele frequency of at least 90% (assuming a homozygous mutation). NEXTGENE software v2.0 (SoftGenetics, State College, PA) was also used to analyze the reads, with a default setting. Variants found by both of the informatics methods were selected. The variants found in common between individuals II-1 and II-2 were focused on, and confirmed as true positives by Sanger sequencing of polymerase chain reaction (PCR) products amplified from patient genomic DNA, except for variants within genes at segmental duplications. The pathological significance of the variants was evaluated using four different websites: POLYPHEN (Polymorphism Phenotyping; http://genetics.bwh.harvard.edu/pph/index.html), POLYPHEN-2 (http://genetics.bwh.harvard.edu/pph2/index.shtml), SIFT (http://sift.jcvi.org/) (output values less than 0.05 are deleterious), and MUTATIONTASTER (http://neurocore.charite.de/MutationTaster/).

### Capillary sequencing

Possible pathological variants were confirmed by Sanger sequencing using an ABI 3500xl or ABI3100 autosequencer (Life Technologies, Carlsbad, CA), following the manufacturer's protocol. Sequencing data were analyzed using SEQUENCHER software (Gene Codes Corporation, Ann Arbor, MI).

### Expression studies

The relative mRNA levels of *TMEM187* in cDNA of various fetal and adult human tissues (Human MTC™ Panel I and Human Fetal MTC™ Panel; Clontech, Mountain View, CA) were determined by quantitative real-time reverse transcription–polymerase chain reaction (RT-PCR) using TaqMan gene expression assays (Hs01920894_s1 for *TMEM187* and Hs00357333_g1 for β-actin as a control) (Life Technologies).

## Results and discussion

Our coverage analysis indicated that for individuals II-1 and II-2, 79.2% and 78.8%, respectively, of the entire X-chromosome coding sequence (CDS) were completely covered, and 88.5% and 88.5%,

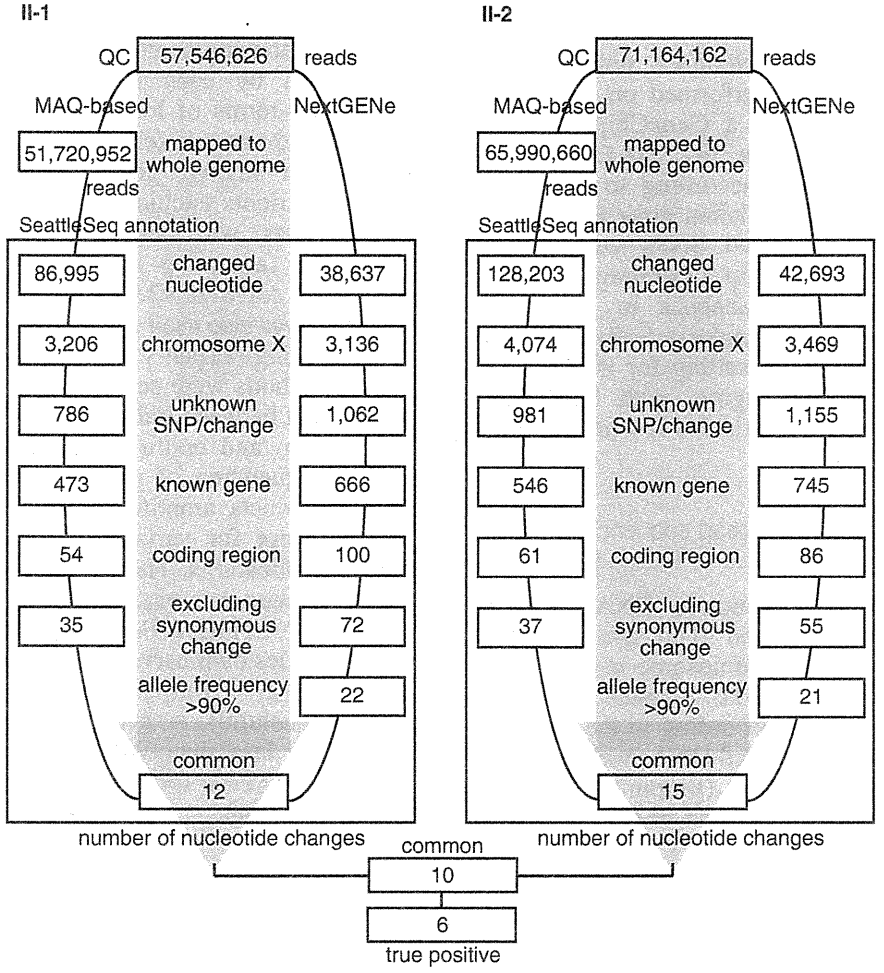


*Fig.* 2. Flow of informatics analysis. A MAQ-based method and NextGENe analysis were performed in individuals II-1 and II-2. The selection methods employed included variants compared with the human genome reference sequence, variants mapped to chromosome X, unknown variants [excluding registered single-nucleotide polymorphisms (SNPs)], variants in known genes, variants in coding regions, variants excluding synonymous changes, and variants common to the two informatics methods. Finally, the nucleotide changes in common between individuals II-1 and II-2 were focused on as potentially pathogenic mutations. True positive changes were confirmed by capillary sequencing of polymerase chain reaction (PCR) products amplified from genomic DNA.

respectively, of the CDS were at least 90% covered by reads. Using a single lane of sequencing per sample, the coverage with 20 reads or more comprised 89.6% and 89.7% of the CDS, and that with 100 reads or more comprised 87.6% and 89.7% of the CDS in individuals II-1 and II-2, respectively. SNP genotyping indicated that the region from rs727240 to rs721003 (UCSC genome browser hg19 assembly, chromosome X coordinates: 22131639–54454152; 32.2 Mb) was unlinked to the phenotype. Exome sequencing using two informatics methods successfully identified six potentially interesting changes as true positives in the linked region: *FAM123B* (RefSeq Gene ID NM_152424): c.85G>A (p.A29T), *FRMD7* (NM_194277): c.875T>C (p.L292P), *L1CAM* (NM_000425): c.92T>C (p.V31A), *TMEM187* (NM_003492): c.334G>A (p.A112T), *FLNA* (NM_001110556): c.1582G>A (p.V528M), and *LAGE3* (NM_006014): c.395G>A (p.R132Q).

The c.92T>C (p.V31A) variant in *L1CAM* was previously found in a patient with Hirschsprung disease, acrocallosal syndrome, and congenital hydrocephalus (8). *L1CAM* mutations cause a wide variety of clinical phenotypes: hydrocephalus due to stenosis of the aqueduct of Sylvius (MIM #307000), MASA syndrome (mental retardation, aphasia, shuffling gait, adducted thumb; MIM #303350), and X-linked agenesis of the corpus callosum (MIM #217990). Phenotypic variability, even within a family, has been noted, raising the caution that definite clinical diagnosis in single

Table 1. Characterization of nucleotide changes found by exome sequencing

| | *FAM123B* | *FRMD7* | *L1CAM* | *TMEM187* | *FLNA* | *LAGE3* |
|---|---|---|---|---|---|---|
| Change | c.85G>A (p.A29T) | c.875T>C (p.L292P) | c.92T>C (p.V31A) | c.334G>A (p.A112T) | c.1582G>A (p.V528M) | c.395G>A (p.R132Q) |
| PolyPhen | Benign | Probably damaging | Benign | Benign | Possibly damaging | Benign |
| PolyPhen-2 | Probably damaging | Probably damaging | Benign | Possibly damaging | Possibly damaging | Possibly damaging |
| SIFT | 0.04 | 0.02 | 0.22 | 0.02 | 0.04 | 0.46 |
| MutationTaster | Polymorphism | Disease causing | Disease causing | Polymorphism | Polymorphism | Polymorphism |
| Normal female | 8/502[a] | 2/502 | 2/502 | 1/502 | 15/502[a] | 4/502 |
| Normal male | 1/118 | 0/117 | 0/118 | 0/118 | | 1/86 |
| Note | | No nystagmus in II-2 | | | | |

[a]Including one homozygous female. Underlining means that this result excludes the variant as potentially causative. Grayed shading indicates the variants that could not be excluded; between these two, the *L1CAM* variant is more likely to be causative.

cases is often impossible (9). Phenotypic features compatible with the *L1CAM* mutation in our patients include spastic paralysis, aphasia, severe mental and growth retardation, but atypical leukodystrophy and the absence of adducted thumbs were very rare or exceptional (9). A normal control study found that 2 of 251 normal females were heterozygous for this SNP, but none of 117 normal males carried the variant allele. One of the four web-based analyses of pathological significance (MutationTaster) indicated that this variant would be disease causing, while the others indicated that it would be benign (Table 1). X-linked hydrocephalus due to *L1CAM* mutations occurs in approximately 1/30 000 male births (10). Considering that the *L1CAM* mutation was found in 2/618 control alleles (0.32%), the change may be a rare polymorphism, a mutation causing lethality in the majority of affected males, or a mutation with low penetrance. Because we were unable to exclude this *L1CAM* change, its pathogenic status remains inconclusive.

We next examined c.85G>A in *FAM123B*, c.875T>C in *FRMD7*, c.1582G>A in *FLNA*, and c.395G>A in *LAGE3* in normal controls. The *FAM123B*, *FLNA*, and *LAGE3* variants were excluded as causative because a homozygous change was found in 1 of 251 female controls (*FAM123B* and *FLNA*) or a hemizygous change was found in 1 of 86 normal males (*LAGE3*). However, the thick calvarium in individuals II-1 and II-2 may be influenced by the *FAM123B* change, because it is causative for osteopathia striata with cranial sclerosis, an X-linked dominant disorder (MIM #300373) (11, 12). As the calvarium of the patients' mother having the heterozygous *FAM123B* change was not evaluated by CT, we could not confirm this possibility.

Only 2 of 251 control females carried the c.875T>C variant in *FRMD7* heterozygously, and none of 117 male controls carried this variant; thus, the pathogenicity of the *FMRD7* variant was inconclusive. Other *FRMD7* mutations cause X-linked congenital nystagmus 1 (MIM #310700) (13). However, the nystagmus found in individual II-1 was not observed in individual II-2, indicating that the variant in common between two brothers did not consistently cause nystagmus. Thus, it may not contribute to the phenotype in this family (Table 1).

We also evaluated the c.334G>A variant in *TMEM187*. Only 2 of 251 female controls carried this heterozygous change, and it was not found among 118 male controls. Two of the four programs (PolyPhen-2 and SIFT) indicated that it would be pathogenic. By Taqman assay, *TMEM187* was ubiquitously expressed in various fetal and adult tissues, including the brain (data not shown), leaving the effect of this mutation on the phenotype in these patients inconclusive (Table 1).

In conclusion, we found two possible but inconclusive variants in this family with two boys affected by atypical leukodystrophy. High-throughput technologies are clearly powerful to detect genomic changes, but evaluation of the data can be very difficult and should be performed cautiously. More knowledge of rare SNPs and mutations is absolutely necessary before any conclusions can be drawn.

## Acknowledgements

We would like to thank the patients and their family members for their participation in this study. This work was supported by research grants from the Ministry of Health, Labour and Welfare

(to H. S., N. Miyake, and N. Matsumoto), the Japan Science and Technology Agency (to N. Matsumoto), a Grant-in-Aid for Scientific Research from the Japan Society for the Promotion of Science (to N. Matsumoto), and a Grant-in-Aid for Young Scientists from the Japan Society for the Promotion of Science (to H. D., N. Miyake, and H. S.).

## References

1. Saitsu H, Kato M, Mizuguchi T et al. De novo mutations in the gene encoding STXBP1 (MUNC18-1) cause early infantile epileptic encephalopathy. Nat Genet 2008: 40: 782–788.
2. Check Hayden E. Genomics shifts focus to rare diseases. Nature 2009: 461: 458.
3. Biesecker LG. Exome sequencing makes medical genomics a reality. Nat Genet 2010: 42: 13–14.
4. Kuhlenbaumer G, Hullmann J, Appenzeller S. Novel genomic techniques open new avenues in the analysis of monogenic disorders. Hum Mutat 2011: 32: 144–151.
5. Miyake N, Kosho T, Mizumoto S et al. Loss-of-function mutations of CHST14 in a new type of Ehlers-Danlos syndrome. Hum Mutat 2010: 31: 966–974.
6. Ng SB, Bigham AW, Buckingham KJ et al. Exome sequencing identifies MLL2 mutations as a cause of Kabuki syndrome. Nat Genet 2010: 42: 790–793.
7. Li H, Ruan J, Durbin R. Mapping short DNA sequencing reads and calling variants using mapping quality scores. Genome Res 2008: 18: 1851–1858.
8. Nakakimura S, Sasaki F, Okada T et al. Hirschsprung's disease, acrocallosal syndrome, and congenital hydrocephalus: report of 2 patients and literature review. J Pediatr Surg 2008: 43: E13–E17.
9. Rietschel M, Friedl W, Uhlhaas S, Neugebauer M, Heimann D, Zerres K. MASA syndrome: clinical variability and linkage analysis. Am J Med Genet 1991: 41: 10–14.
10. Rosenthal A, Jouet M, Kenwrick S. Aberrant splicing of neural cell adhesion molecule L1 mRNA in a family with X-linked hydrocephalus. Nat Genet 1992: 2: 107–112.
11. Viot G, Lacombe D, David A et al. Osteopathia striata cranial sclerosis: non-random X-inactivation suggestive of X-linked dominant inheritance. Am J Med Genet 2002: 107: 1–4.
12. Jenkins ZA, van Kogelenberg M, Morgan T et al. Germline mutations in WTX cause a sclerosing skeletal dysplasia but do not predispose to tumorigenesis. Nat Genet 2009: 41: 95–100.
13. Tarpey P, Thomas S, Sarvananthan N et al. Mutations in FRMD7, a newly identified member of the FERM family, cause X-linked idiopathic congenital nystagmus. Nat Genet 2006: 38: 1242–1244.

RESEARCH ARTICLE

AMERICAN JOURNAL OF medical genetics PART A

# Submicroscopic Deletion of 12q13 Including *HOXC* Gene Cluster With Skeletal Anomalies and Global Developmental Delay

**Nobuhiko Okamoto,[1]* Daisuke Tamura,[2] Gen Nishimura,[3] Keiko Shimojima,[4] and Toshiyuki Yamamoto[4]**

[1]Department of Medical Genetics, Osaka Medical Center and Research Institute for Maternal and Child Health, Osaka, Japan

[2]Department of Orthopedics, Osaka Medical Center and Research Institute for Maternal and Child Health, Osaka, Japan

[3]Department of Pediatric Imaging, Tokyo Metropolitan Children's Medical Center, Tokyo, Japan

[4]Tokyo Women's Medical University Institute for Integrated Medical Sciences, Tokyo, Japan

Received 13 May 2011; Accepted 4 September 2011

We report on a patient with a submicroscopic deletion of 12q13 detected by array-CGH and confirmed by FISH. He was haploinsufficient for the *HOXC* gene cluster and some other neighboring genes. *HOX* genes have an important role in the initial formation of the body. The patient showed characteristic features including severe kyphoscoliosis, digital abnormalities, cardiac anomaly, expressive language, and global developmental delay. Radiologic features of the fingers had some similarities with those for multiple synostosis syndrome. No human genetic disorders due to *HOXC* abnormalities are yet known. We tentatively assume that his skeletal anomalies are associated with haploinsufficiency of the *HOXC* gene cluster. Further studies are necessary to determine the clinical importance of haploinsufficiency of the *HOXC* gene cluster. 

**Key words:** *HOX*; *HOXC*; array-CGH; kyphoscoliosis; multiple synostosis syndrome

**How to Cite this Article:**
Okamoto N, Tamura D, Nishimura G, Shimojima K, Yamamoto T. 2011. Submicroscopic deletion of 12q13 including *HOXC* gene cluster with skeletal anomalies and global developmental delay.
Am J Med Genet Part A 155:2997–3001.

## INTRODUCTION

*HOX* genes have an important role in the initial formation of the body plan by providing positional information along the anterior–posterior body and limb axis and are associated with neural tube closure. *HOX* A, B, C, and D make a cluster on chromosomes 7, 17, 12, and 2, respectively. Each cluster consists of 9–11 genes from 13 paralogous groups. The order of the *HOX* genes along the chromosome correlates with their expression along the anterior/posterior axis of the embryo.

Some of the *HOX* genes are associated with genetic syndromes. Akarsu et al. [1996] reported that a polyalanine tract expansion in *HOXD13* causes synpolydactyly (OMIM #186000). Mortlock and Innis [1997] found a nonsense mutation in *HOXA13* among patients with hand-foot-genital syndrome (OMIM #140000). Thompson and Nguyen [2000] reported that megakaryocytic thrombocytopenia and radio-ulnar synostosis (OMIM #605432) are associated with *HOXA11* mutations. Shrimpton et al. [2004] reported a *HOXD10* mutation in a family with isolated congenital vertical talus and Charcot-Marie-Tooth disease (OMIM #142984). Tischfield et al. [2005] identified homozygous truncating mutations in *HOXA1* in patients with horizontal gaze abnormalities, deafness, facial weakness, hypoventilation, vascular malformations of the internal carotid arteries and cardiac outflow tract, intellectual disability, and autism spectrum disorder. Two syndromes associated with homozygous mutations of *HOXA1* are known as the Bosley-Salih-Alorainy syndrome and the Athabascan brainstem dysgenesis syndrome (OMIM #601536) [Bosley et al., 2008]. Alasti et al. [2008] reported a mutation in *HOXA2* in autosomal-recessive microtia (OMIM #612290).

Spitz et al. [2002] reported a t(2;8)(q31;p21) balanced translocation with breakpoints near the human *HOXD* complex. The patient had mesomelic dysplasia of the upper limbs and vertebral defects. Dlugaszewska et al. [2006] reported three patients with limb abnormalities and breakpoints involving chromosome 2q31. None of the three 2q31 breakpoints, which all mapped close to the *HOXD*

Additional supporting information may be found in the online version of this article.

Grant sponsor: Ministry of Health, Labour, and Welfare in Japan.

*Correspondence to:
Dr. Nobuhiko Okamoto, Department of Medical Genetics, Osaka Medical Center and Research Institute for Maternal and Child Health, 840 Murodo-cho, Izumi, Osaka 594-1101, Japan. E-mail: okamoto@osaka.email.ne.jp

Published online 8 November 2011 in Wiley Online Library (wileyonlinelibrary.com).
DOI 10.1002/ajmg.a.34324

cluster, disrupted any known genes. They suggested that the three rearrangements disturb normal *HOXD* gene regulation by position effects. Yue et al. [2007] reported a boy with severe intellectual disability, funnel chest, bell-shaped thorax, and hexadactyly of both feet. The patient had a balanced de novo t(12;17)(p13.3;q21.3) translocation. The breakpoint was near the *HOXB* cluster. They proposed that misregulation of a *HOXB* gene(s) by position effect is responsible for the patient's phenotype. Jun et al. [2011] reported a patient with the *HOXA* cluster deletion with manifestations similar to those observed in hand-foot-genital syndrome, which is caused by a haploinsufficiency of *HOXA13*.

We report on a patient with distinctive skeletal anomalies with a submicroscopic deletion of 12q13. He was haploinsufficient for the *HOXC* gene cluster. So far, no human genetic disorders due to *HOXC* abnormalities are reported. We discuss the clinical features in the patient and the haploinsufficiency of the *HOXC* genes.

## CLINICAL REPORT

The 14-year-old male propositus was the first-born child of a 26-year-old mother and a 30-year-old father, both healthy and non-consanguineous. After an uncomplicated pregnancy, he was born at 39 weeks of gestation by induced delivery. His length was 53 cm (90th centile). His birth weight was 3,010 g, within normal limits (25th centile). After birth, cardiac murmur was noticed. Echocardiography revealed tetralogy of Fallot. Cardiac surgery was carried out successfully at 2 years of age. Surgery for bilateral inguinal hernia and strabismus was done at 3 years of age. His dentition was abnormal. Persistent teeth erupted before the loss of primary teeth. He showed hypodontia.

His development was delayed since early infancy. From the age of 6 months, he received physical training for delayed motor development. He was able to roll over at 10 months of age, and to sit alone at 3 years of age. He started to walk independently at 5 years of age and the spine deformity appeared. His global development quotient was 20 at 3 years of age. He attended special education in school. Gradually, he could understand simple words. His intellectual quotient remained around 30 and verbal production was almost absent. However, recently he could express simple sentences using key boards.

Physical examination identified dysmorphic features, including a long face, a broad nose, prominent ears, bilateral low-set ears, downslanting palpebral fissures and a high palate. Severe kyphosis and mild scoliosis were remarkable features. The radial heads were dislocated bilaterally. Camptodactyly of middle and ring fingers, inflexible distal interphalangeal joints of index fingers and adducted thumbs of both hands were noted (Fig. 1A). Hearing and visual acuity were normal. His weight was 29 kg (<3rd centile), and his length was 160 cm (<3rd centile). His head circumference was average for his age, 14 years.

Radiographic analysis revealed severe kyphosis and mild scoliosis in the thoracic spine (Fig. 2A,B). The upper thorax was mildly narrowed. The proximal interphalangeal joints of both the middle and ring fingers showed flexion contracture with para-articular swelling (Fig. 1B). The proximal interphalangeal joints of both index fingers were swollen as well. The metacarpophalangeal joint of the right index finger and proximal interphalangeal joint of the left little finger showed ulnar deviation. The metacarpals were mildly undertubulated. Radiologic features of the fingers were like those seen in multiple synostosis syndrome. However, no carpal or tarsal coalition was found.

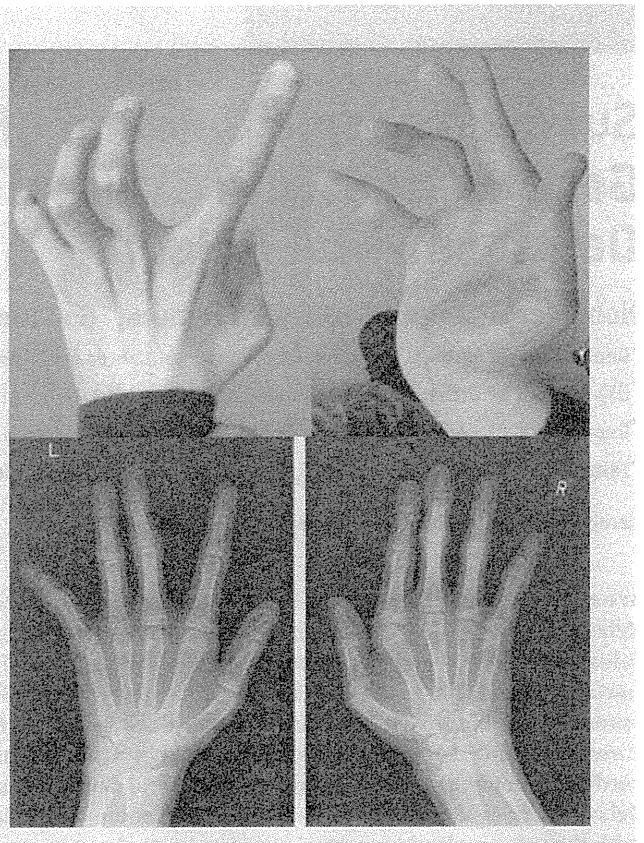


**FIG. 1. A: Hands of the patient showing camptodactyly of middle and ring fingers, inflexible distal interphalangeal joints of index fingers and adducted thumbs of both hands. B: Radiograph of the hands. The proximal interphalangeal joints of both middle and ring fingers show flexion contracture with para-articular swelling.**

Results of neuroradiological examinations including brain CT and MRI were normal. Routine laboratory tests were normal. His karyotype by G-banded analysis was 46,XY. Array-CGH analyses were performed to look for submicroscopic chromosomal aberrations.

## MATERIALS AND METHODS

After obtaining informed consent and the permission of the institution's ethics committee, peripheral blood samples were drawn from the patient and his parents. Genomic DNA was extracted using the QIAquick DNA extraction kit (Qiagen, Valencia, CA).

Based on the hypothesis that the patient might have submicroscopic chromosomal aberrations, array-CGH analysis was performed using the Human Genome CGH Microarray 60K (Agilent Technologies, Santa Clara, CA) as described previously [Shimojima et al., 2009].

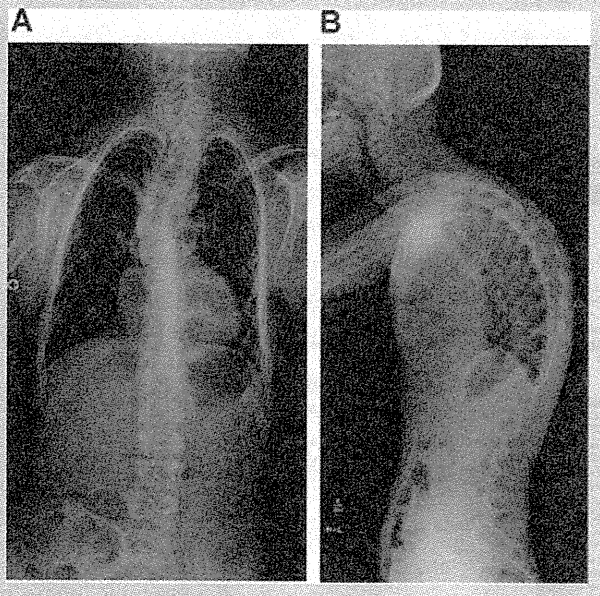


FIG. 2. Radiographs of the spine. A: Frontal view showing severe kyphosis and mild scoliosis in the thoracic spine. The upper thorax is mildly narrow. B: Lateral view.

Metaphase nuclei were prepared from peripheral blood lymphocytes by standard methods and used for FISH with human BAC clones selected from the UCSC genome browser (http://www.genome.ucsc.edu) as described elsewhere [Shimojima et al., 2009]. Physical positions refer to the March 2006 human reference sequence (NCBI Build 36.1).

## RESULTS

By array-CGH analysis, loss of genomic copy numbers was identified in the region 12q13, which included the *HOXC* cluster (Fig. 3). The size of the deletion was 1.7 Mb. FISH analyses confirmed the deletion (see Supplementary Fig. A). FISH analyses of the parents found the deletion was de novo (data not shown). The karyotype of the patient was arr 12q13.1 (51,965,307-53,642,659)×1 dn.

## DISCUSSION

A patient with distinctive skeletal anomalies had a submicroscopic deletion of 12q13 including *HOXC* gene cluster. His features included tetralogy of Fallot, abnormal dentition, and global developmental delay. This is the first report of *HOXC* gene cluster deletion. Human genetic disorders due to *HOXC* abnormalities are not known.

There have been multiple knock out studies on *Hoxc* genes. *Hoxc-4* is expressed in the most anterior regions of the CNS and prevertebral column. *Hoxc-4* mutant (−/−) mice showed a partial posterior homeotic transformation of the 7th cervical vertebra [Saegusa et al., 1996]. In addition, anterior transformations of the 3rd and 8th thoracic vertebrae, and an aperture or a fissure in the xiphoid process of the sternum were observed. No obvious defects were observed in the CNS. *Hoxc-4* (−/−) mice manifested vertebral defects that extended from the 2nd to 11th thoracic vertebra and died because of esophageal stenosis [Boulet and Capecchi, 1996].

*Hoxc-8* is expressed in the limbs, backbone rudiments, and neural tube of mouse midgestation embryos, and in the cartilage and skeleton of newborns. Le Mouellic et al. [1992] generated *Hoxc-8* (−/−) mice. The mice were born alive, but most of them died within a few days. Anterior transformation in the several skeletal segments was characteristic. The 8th pair of ribs attached to the sternum and the 14th pair of ribs appeared on the 1st lumbar vertebra. During embryogenesis, *Hoxc-8* is highly expressed in motoneurons within spinal cord segments C7 to T1. These motoneurons innervate forelimb distal muscles that move the forepaw. *Hoxc-8*-deficient mice showed a congenital prehension deficiency of the forepaw due to abnormal innervation [Tiret et al., 1998].

Suemori et al. [1995] generated *Hoxc-9* mutant mice. Homozygous mice showed an anterior homeotic transformation from the 10th thoracic vertebra to the first lumbar vertebra. Bending and fusion of the ribs were observed. Eight or nine pairs of ribs were attached to the sternum. The sternum showed an abnormal pattern of ossification. Phenotypes of the mutant mice resembled those of the *Hoxc-8* mutant mice. Functional interaction between *Hoxc-8* and *Hoxc-9* during segmental determination was suspected.

Godwin and Capecchi [1998] reported *Hoxc-13* expression in the nails, tail, vibrissae, and filiform papillae of the tongue, and in hair follicles throughout the body. Mice homozygous for mutant alleles of *Hoxc-13* show brittle hair resulting in alopecia.

Suemori and Noguchi [2000] produced *Hox C* cluster null (−/−) mice. These mice die soon after birth with minor transformations. Perinatal death of the *HoxC* cluster (−/−) mutant mice is thought to be attributable to a neuromuscular defect in respiratory organs. Gross appearance of the skeleton and internal organs was almost normal. The mutant mouse showed subtle vertebral and rib anomalies. Malformations in the skeleton were even milder than those observed in some single gene mutant mice of *HoxC* genes. This means that at least some genes within a cluster interact with each other. The phenotype of *HoxC* cluster (+/−) mice, which have a similar genetic condition to our patient, was normal.

The phenotype of knockout mice does not always correspond to human disorders. Skeletal manifestations in our patient were not evident in his early childhood. Skeletal changes may progress during growth. Interestingly, translocation breakpoint near *HOXB* and *HOXD* with positional effect caused thoracic deformities and digital abnormalities [Spitz et al., 2002; Dlugaszewska et al., 2006; Yue et al., 2007]. We tentatively assume that skeletal anomalies in our patient are associated with haploinsufficiency of the *HOXC* gene cluster.

Radiologic features of the fingers had some similarities with those for multiple synostosis syndrome (OMIM #186500). Shi et al. [1999] found that Smad1 dislodges Hoxc-8 from its DNA-binding element and result in the induction of gene expression. Bone morphogenetic proteins (BMPs) induce osteoblast differentiation and bone formation. Smad1 mediates signaling initiated by BMPs and activates osteopontin and osteoprotegerin gene expression by dislodging Hoxc-8 from its DNA-binding sites [Liu et al., 2004].

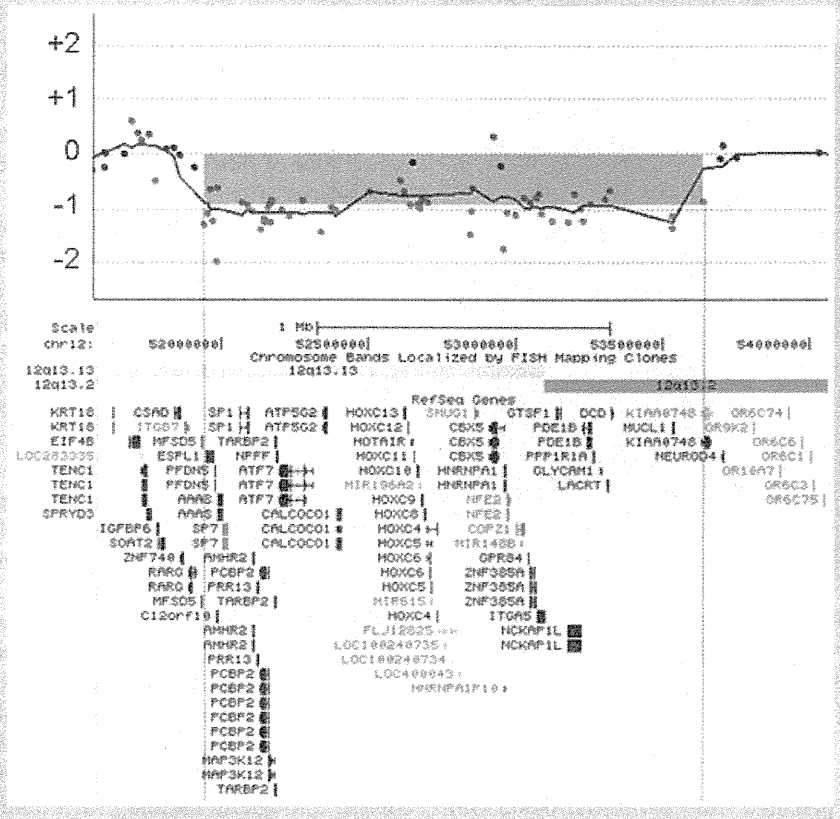


FIG. 3. Array-CGH revealed a loss of genomic copy numbers in the region 12q13, which included the *HOXC* cluster.

These findings indicate that *HOXC8* deficiency may induce osteogenesis by activating osteopontin and osteoprotegerin. The manifestations similar to the multiple synostosis syndrome, the flexion contracture and other digital abnormalities in our patient, may have some association with the *HOXC8* haploinsufficiency.

The multiple genes involved in the deletion may contribute to the manifestations. Our patient was haploinsuffient for *SP7/OSX*, *AAAS*, and *AMHRII*. Lapunzina et al. [2010] reported a homozygous single base pair deletion (c.1052delA) in *SP7/OSX* in an Egyptian child with recessive osteogenesis imperfecta (OMIM #613849). *SP7/OSX* plays a key role in human bone development. The triple-A syndrome (OMIM #231550) is caused by mutation in the gene-encoding aladin (*AAAS*; OMIM 605378). The anti-Müllerian hormone type II (AMHRII) receptor is the primary receptor for anti-Müllerian hormone (AMH), a protein responsible for the regression of the Müllerian duct in males. Mutations in the *AMHRII* gene lead to persistent Müllerian duct syndrome (OMIM #261550) in human males [Belville et al., 2009]. These syndromes are transmitted in autosomal recessive fashion and are not responsible for the manifestations in our patient. A haploinsufficiency of other genes may contribute to cardiac anomalies, dental anomalies, and intellectual disability with severe expressive language delay. Some of the deleted genes including *GPR84*, *PDE1B*, and *NPFF* are expressed in the nervous system. However, contribution of these genes to language development is unclear.

In conclusion, we report on a patient with distinctive skeletal anomalies and intellectual disability with a submicroscopic deletion of 12q13 including *HOXC* gene cluster. No human genetic disorders due to *HOXC* abnormalities are yet known. We posit that his kyphoscoliosis and digital abnormalities may be associated with haploinsufficiency of the *HOXC* gene cluster. Further studies of patients with similar conditions are necessary to determine the clinical significance of haploinsufficiency of the *HOXC* gene cluster.

## ACKNOWLEDGMENTS

We thank for the family for their cooperation. This study was supported by the Health and Labour Research Grants in 2010 by Ministry of Health, Labour and Welfare in Japan.

## REFERENCES

Akarsu AN, Stoilov I, Yilmaz E, Sayli BS, Sarfarazi M. 1996. Genomic structure of HOXD13 gene: A nine polyalanine duplication causes synpolydactyly in two unrelated families. Hum Mol Genet 5:945–952.

Alasti F, Sadeghi A, Sanati MH, Farhadi M, Stollar E, Somers T, Van Camp G. 2008. A mutation in HOXA2 is responsible for autosomal-recessive microtia in an Iranian family. Am J Hum Genet 82:982–991.

Belville C, Maréchal JD, Pennetier S, Carmillo P, Masgrau L, Messika-Zeitoun L, Galey J, Machado G, Treton D, Gonzalès J, Picard JY, Josso N, Cate RL, di Clemente N. 2009. Natural mutations of the anti-Mullerian hormone type II receptor found in persistent Mullerian duct syndrome affect ligand binding, signal transduction and cellular transport. Hum Mol Genet 18:3002–3013.

Bosley TM, Alorainy IA, Salih MA, Aldhalaan HM, Abu-Amero KK, Oystreck DT, Tischfield MA, Engle EC, Erickson RP. 2008. The clinical spectrum of homozygous HOXA1 mutations. Am J Med Genet A 146A:1235–1240.

Boulet AM, Capecchi MR. 1996. Targeted disruption of hoxc-4 causes esophageal defects and vertebral transformations. Dev Biol 177:232–249.

Dlugaszewska B, Silahtaroglu A, Menzel C, Kübart S, Cohen M, Mundlos S, Tümer Z, Kjaer K, Friedrich U, Ropers HH, Tommerup N, Neitzel H, Kalscheuer VM. 2006. Breakpoints around the HOXD cluster result in various limb malformations. J Med Genet 43:111–118.

Godwin AR, Capecchi MR. 1998. Hoxc13 mutant mice lack external hair. Genes and Dev 12:11–20.

Jun KR, Seo EJ, Lee JO, Yoo HW, Park IS, Yoon HK. 2011. Molecular cytogenetic and clinical characterization of a patient with a 5.6-Mb deletion in 7p15 including HOXA cluster. Am J Med Genet Part A 155A:642–647.

Lapunzina P, Aglan M, Temtamy S, Caparrós-Martín JA, Valencia M, Letón R, Martínez-Glez V, Elhossini R, Amr K, Vilaboa N, Ruiz-Perez VL. 2010. Identification of a frameshift mutation in Osterix in a patient with recessive osteogenesis imperfecta. Am J Hum Genet 87:110–114.

Le Mouellic H, Lallemand Y, Brûlet P. 1992. Homeosis in the mouse induced by a null mutation in the Hox-3.1 gene. Cell 69:251–264.

Liu Z, Shi W, Ji X, Sun C, Jee WS, Wu Y, Mao Z, Nagy TR, Li Q, Cao X. 2004. Molecules mimicking Smad1 interacting with Hox stimulate bone formation. J Biol Chem 279:11313–11319.

Mortlock DP, Innis JW. 1997. Mutation of HOXA13 in hand-foot-genital syndrome. Nat Genet 15:179–180.

Saegusa H, Takahashi N, Noguchi S, Suemori H. 1996. Targeted disruption in the mouse Hoxc-4 locus results in axial skeleton homeosis and malformation of the xiphoid process. Dev Biol 174:55–64.

Shi X, Yang X, Chen D, Chang Z, Cao X. 1999. Smad1 interacts with homeobox DNA-binding proteins in bone morphogenetic protein signaling. J Biol Chem 274:13711–13717.

Shimojima K, Páez MT, Kurosawa K, Yamamoto T. 2009. Proximal interstitial 1p36 deletion syndrome: The most proximal 3.5-Mb microdeletion identified on a dysmorphic and mentally retarded patient with inv(3)(p14.1q26.2). Brain and Development 31:629–633.

Shrimpton AE, Levinsohn EM, Yozawitz JM, Packard DS Jr, Cady RB, Middleton FA, Persico AM, Hootnick DR. 2004. A HOX gene mutation in a family with isolated congenital vertical talus and Charcot-Marie-Tooth disease. Am J Hum Genet 75:92–96.

Spitz F, Montavon T, Monso-Hinard C, Morris M, Ventruto ML, Antonarakis S, Ventruto V, Duboule D. 2002. A t(2;8) balanced translocation with breakpoints near the human HOXD complex causes mesomelic dysplasia and vertebral defects. Genomics 79:493–498.

Suemori H, Noguchi S. 2000. Hox C cluster genes are dispensable for overall body plan of mouse embryonic development. Dev Biol 220:333–342.

Suemori H, Takahashi N, Noguchi S. 1995. Hoxc-9 mutant mice show anterior transformation of the vertebrae and malformation of the sternum and ribs. Mech Dev 51:265–273.

Thompson AA, Nguyen LT. 2000. Amegakaryocytic thrombocytopenia and radio-ulnar synostosis are associated with HOXA11 mutation. Nat Genet 26:397–398.

Tiret L, Le Mouellic H, Maury M, Bru?let P. 1998. Increased apoptosis of motoneurons and altered somatotopic maps in the brachial spinal cord of Hoxc-8-deficient mice. Development 125:279–291.

Tischfield MA, Bosley TM, Salih MA, Alorainy IA, Sener EC, Nester MJ, Oystreck DT, Chan WM, Andrews C, Erickson RP, Engle EC. 2005. Homozygous HOXA1 mutations disrupt human brainstem, inner ear, cardiovascular and cognitive development. Nat Genet 37:1035–1037.

Yue Y, Farcas R, Thiel G, Bommer C, Grossmann B, Galetzka D, Kelbova C, Küpferling P, Daser A, Zechner U, Haaf T. 2007. De novo t(12;17)(p13.3;q21.3) translocation with a breakpoint near the 5' end of the HOXB gene cluster in a patient with developmental delay and skeletal malformations. Eur J Hum Genet 15:570–577.

Journal of Human Genetics (2011) 56, 110–124

www.nature.com/jhg

ORIGINAL ARTICLE

# Clinical application of array-based comparative genomic hybridization by two-stage screening for 536 patients with mental retardation and multiple congenital anomalies

Shin Hayashi[1,2], Issei Imoto[1,3], Yoshinori Aizu[4], Nobuhiko Okamoto[5], Seiji Mizuno[6], Kenji Kurosawa[7], Nana Okamoto[1,8], Shozo Honda[1], Satoshi Araki[9], Shuki Mizutani[9], Hironao Numabe[10], Shinji Saitoh[11], Tomoki Kosho[12], Yoshimitsu Fukushima[12], Hiroshi Mitsubuchi[13], Fumio Endo[13], Yasutsugu Chinen[14], Rika Kosaki[15], Torayuki Okuyama[15], Hirotaka Ohki[16], Hiroshi Yoshihashi[17], Masae Ono[18], Fumio Takada[19], Hiroaki Ono[20], Mariko Yagi[21], Hiroshi Matsumoto[22], Yoshio Makita[23], Akira Hata[24] and Johji Inazawa[1,25]

**Recent advances in the analysis of patients with congenital abnormalities using array-based comparative genome hybridization (aCGH) have uncovered two types of genomic copy-number variants (CNVs); pathogenic CNVs (pCNVs) relevant to congenital disorders and benign CNVs observed also in healthy populations, complicating the screening of disease-associated alterations by aCGH. To apply the aCGH technique to the diagnosis as well as investigation of multiple congenital anomalies and mental retardation (MCA/MR), we constructed a consortium with 23 medical institutes and hospitals in Japan, and recruited 536 patients with clinically uncharacterized MCA/MR, whose karyotypes were normal according to conventional cytogenetics, for two-stage screening using two types of bacterial artificial chromosome-based microarray. The first screening using a targeted array detected pCNV in 54 of 536 cases (10.1%), whereas the second screening of the 349 cases negative in the first screening using a genome-wide high-density array at intervals of approximately 0.7 Mb detected pCNVs in 48 cases (13.8%), including pCNVs relevant to recently established microdeletion or microduplication syndromes, CNVs containing pathogenic genes and recurrent CNVs containing the same region among different patients. The results show the efficient application of aCGH in the clinical setting.**
*Journal of Human Genetics* (2011) **56**, 110–124; doi:10.1038/jhg.2010.129; published online 28 October 2010

**Keywords:** array-CGH; congenital anomaly; mental retardation; screening

## INTRODUCTION

Mental retardation (MR) or developmental delay is estimated to affect 2–3% of the population.[1] However, in a significant proportion of cases, the etiology remains uncertain. Hunter[2] reviewed 411 clinical cases of MR and reported that a specific genetic/syndrome diagnosis was carried out in 19.9% of them. Patients with MR often have congenital anomalies, and more than three minor anomalies can be useful in the diagnosis of syndromic MR.[2,3] Although chromosomal aberrations are well-known causes of MR, their frequency determined by conventional karyotyping has been reported to range from 7.9 to 36% in patients with MR.[4–8] Although the diagnostic yield depends on the population of each study or clinical conditions, such studies

[1]Department of Molecular Cytogenetics, Medical Research Institute and School of Biomedical Science, Tokyo Medical and Dental University, Tokyo, Japan; [2]Hard Tissue Genome Research Center, Tokyo Medical and Dental University, Tokyo, Japan; [3]Department of Human Genetics and Public Health Graduate School of Medical Science, The University of Tokushima, Tokushima, Japan; [4]Division of Advanced Technology and Development, BML, Saitama, Japan; [5]Department of Medical Genetics, Osaka Medical Center and Research Institute for Maternal and Child Health, Osaka, Japan; [6]Department of Pediatrics, Central Hospital, Aichi Human Service Center, Kasugai, Japan; [7]Division of Medical Genetics, Kanagawa Children's Medical Center, Yokohama, Japan; [8]Department of Maxillofacial Orthognathics, Graduate School, Tokyo Medical and Dental University, Tokyo, Japan; [9]Department of Pediatrics and Developmental Biology, Tokyo Medical and Dental University Graduate School, Tokyo, Japan; [10]Department of Medical Genetics, Kyoto University Hospital, Kyoto, Japan; [11]Department of Pediatrics, Hokkaido University Graduate School of Medicine, Sapporo, Japan; [12]Department of Medical Genetics, Shinshu University School of Medicine, Matsumoto, Japan; [13]Department of Pediatrics, Kumamoto University Graduate School of Medical Science, Kumamoto, Japan; [14]Department of Pediatrics, University of the Ryukyu School of Medicine, Okinawa, Japan; [15]Department of Clinical Genetics and Molecular Medicine, National Center for Child Health and Development, Tokyo, Japan; [16]The Division of Cardiology, Tokyo Metropolitan Children's Medical Center, Tokyo, Japan; [17]The Division of Medical Genetics, Tokyo Metropolitan Children's Medical Center, Tokyo, Japan; [18]Department of Pediatrics, Tokyo Teishin Hospital, Tokyo, Japan; [19]Department of Medical Genetics, Kitasato University Graduate School of Medical Sciences, Sagamihara, Japan; [20]Department of Pediatrics, Hiroshima Prefectural Hospital, Hiroshima, Japan; [21]Department of Pediatrics, Kobe University Graduate School of Medicine, Kobe, Japan; [22]Department of Pediatrics, National Defense Medical College, Saitama, Japan; [23]Education Center, Asahikawa Medical College, Asahikawa, Japan; [24]Department of Public Health, Chiba University Graduate School of Medicine, Chiba, Japan and [25]Global Center of Excellence (GCOE) Program for 'International Research Center for Molecular Science in Tooth and Bone Diseases', Tokyo Medical and Dental University, Tokyo, Japan
Correspondence: Professor J Inazawa, Department of Molecular Cytogenetics, Medical Research Institute, Tokyo Medical and Dental University, 1-5-45 Yushima, Bunkyo-ku, Tokyo 113-8510, Japan.
E-mail: johinaz.cgen@mri.tmd.ac.jp
Received 20 August 2010; revised 25 September 2010; accepted 30 September 2010; published online 28 October 2010

suggest that at least three quarters of patients with MR are undiagnosed by clinical dysmorphic features and karyotyping.

In the past two decades, a number of rapidly developed cytogenetic and molecular approaches have been applied to the screening or diagnosis of various congenital disorders including MR, congenital anomalies, recurrent abortion and cancer pathogenesis. Among them, array-based comparative genome hybridization (aCGH) is used to detect copy-number changes rapidly in a genome-wide manner and with high resolution. The target and resolution of aCGH depend on the type and/or design of mounted probes, and many types of microarray have been used for the screening of patients with MR and other congenital disorders: bacterial artificial chromosome (BAC)-based arrays covering whole genomes,[9,10] BAC arrays covering chromosome X,[11,12] a BAC array covering all subtelomeric regions,[13] oligonucleotide arrays covering whole genomes,[14,15] an oligonucleotide array for clinical diagnosis[16] and a single nucleotide polymorphism array covering the whole genome.[17] Because genome-wide aCGH has led to an appreciation of widespread copy-number variants (CNVs) not only in affected patients but also in healthy populations,[18–20] clinical cytogenetists need to discriminate between CNVs likely to be pathogenic (pathogenic CNVs, pCNVs) and CNVs less likely to be relevant to a patient's clinical phenotypes (benign CNVs, bCNVs).[21] The detection of more CNVs along with higher-resolution microarrays needs more chances to assess detected CNVs, resulting in more confusion in a clinical setting.

We have applied aCGH to the diagnosis and investigation of patients with multiple congenital anomalies and MR (MCA/MR) of unknown etiology. We constructed a consortium with 23 medical institutes and hospitals in Japan, and recruited 536 clinically uncharacterized patients with a normal karyotype in conventional cytogenetic tests. Two-stage screening of copy-number changes was performed using two types of BAC-based microarray. The first screening was performed by a targeted array and the second screening was performed by an array covering the whole genome. In this study, we diagnosed well-known genomic disorders effectively in the first screening, assessed the pathogenicity of detected CNVs to investigate an etiology in the second screening and discussed the clinical significance of aCGH in the screening of congenital disorders.

## MATERIALS AND METHODS

### Subjects

We constructed a consortium of 23 medical institutes and hospitals in Japan, and recruited 536 Japanese patients with MCA/MR of unknown etiology from July 2005 to January 2010. All the patients were physically examined by an expert in medical genetics or a dysmorphologist. All showed a normal karyotype by conventional approximately 400–550 bands-level G-banding karyotyping. Genomic DNA and metaphase chromosomes were prepared from peripheral blood lymphocytes using standard methods. Genomic DNA from a lymphoblastoid cell line of one healthy man and one healthy woman were used as a normal control for male and female cases, respectively. All samples were obtained with prior written informed consent from the parents and approval by the local ethics committee and all the institutions involved in this project. For subjects in whom CNV was detected in the first or second screening, we tried to analyze their parents as many as possible using aCGH or fluorescence *in situ* hybridization (FISH).

### Array-CGH analysis

Among our recently constructed in-house BAC-based arrays,[22] we used two arrays for this two-stage survey. In the first screening we applied a targeting array, 'MCG Genome Disorder Array' (GDA). Initially GDA version 2, which contains 550 BACs corresponding to subtelomeric regions of all chromosomes except 13p, 14p, 15p, 21p and 22p and causative regions of about 30 diseases already reported, was applied for 396 cases and then GDA version 3, which contains 660 BACs corresponding to those of GDA version 2 and pericentromeric regions of all chromosomes, was applied for 140 cases. This means that a CNV detected by GDA is certainly relevant to the patient's phenotypes. Subsequently in the second screening we applied 'MCG Whole Genome Array-4500' (WGA-4500) that covers all 24 human chromosomes with 4523 BACs at intervals of approximately 0.7 Mb to analyze subjects in whom no CNV was detected in the first screening. WGA-4500 contains no BACs spotted on GDA. If necessary, we also used 'MCG X-tiling array' (X-array) containing 1001 BAC/PACs throughout X chromosome other than pseudoautosomal regions.[12] The array-CGH analysis was performed as previously described.[12,23]

For several subjects we applied an oligonucleotide array (Agilent Human Genome CGH Microarray 244K; Agilent Technologies, Santa Clara, CA, USA) to confirm the boundaries of CNV identified by our in-house BAC arrays. DNA labeling, hybridization and washing of the array were performed according to the directions provided by the manufacturer. The hybridized arrays were scanned using an Agilent scanner (G2565BA), and the CGH Analytics program version 3.4.40 (Agilent Technologies) was used to analyze copy-number alterations after data extraction, filtering and normalization by Feature Extraction software (Agilent Technologies).

### Fluorescence *in situ* hybridization

Fluorescence *in situ* hybridization was performed as described elsewhere[23] using BACs located around the region of interest as probes.

## RESULTS

### CNVs detected in the first screening

In the first screening, of 536 cases subjected to our GDA analysis, 54 (10.1%) were determined to have CNV (Figure 1; Tables 1 and 2).

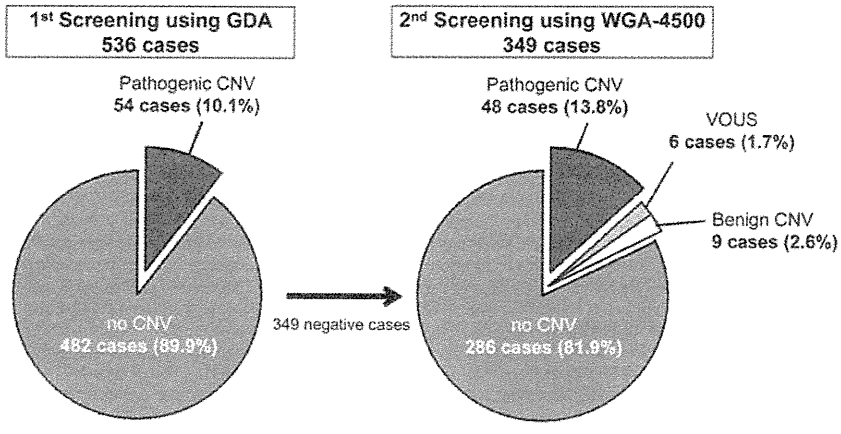


**Figure 1** Percentages of each screening in the current study.